

Search for high-mass diboson resonances with boson-tagged jets in proton-proton collisions at $\sqrt{s} = \text{TeV}$ with the ATLAS detector

著者 (英)	ATLAS Collaboration, Kazuhiko HARA, Shinhong(nobuhiro) KIM, Hideki OKAWA, Koji SATO, Fumihiko UKEGAWA
journal or publication title	Journal of high energy physics
volume	2015
number	12
page range	55
year	2015-12
権利	Open Access, Copyright CERN, for the benefit of the ATLAS Collaboration. Article funded by SCOAP3. This article is distributed under the terms of the Creative Commons Attribution License (CC-BY 4.0), which permits any use, distribution and reproduction in any medium, provided the original author(s) and source are credited.
URL	http://hdl.handle.net/2241/00154104

doi: 10.1007/JHEP12(2015)055

Search for high-mass diboson resonances with boson-tagged jets in proton-proton collisions at $\sqrt{s} = 8$ TeV with the ATLAS detector



The ATLAS collaboration

E-mail: atlas.publications@cern.ch

ABSTRACT: A search is performed for narrow resonances decaying into WW , WZ , or ZZ boson pairs using 20.3 fb^{-1} of proton-proton collision data at a centre-of-mass energy of $\sqrt{s} = 8 \text{ TeV}$ recorded with the ATLAS detector at the Large Hadron Collider. Diboson resonances with masses in the range from 1.3 to 3.0 TeV are sought after using the invariant mass distribution of dijets where both jets are tagged as a boson jet, compatible with a highly boosted W or Z boson decaying to quarks, using jet mass and substructure properties. The largest deviation from a smoothly falling background in the observed dijet invariant mass distribution occurs around 2 TeV in the WZ channel, with a global significance of 2.5 standard deviations. Exclusion limits at the 95% confidence level are set on the production cross section times branching ratio for the WZ final state of a new heavy gauge boson, W' , and for the WW and ZZ final states of Kaluza-Klein excitations of the graviton in a bulk Randall-Sundrum model, as a function of the resonance mass. W' bosons with couplings predicted by the extended gauge model in the mass range from 1.3 to 1.5 TeV are excluded at 95% confidence level.

KEYWORDS: Exotics, Hadron-Hadron Scattering

ARXIV EPRINT: [1506.00962](https://arxiv.org/abs/1506.00962)

Contents

1	Introduction	1
2	ATLAS detector and data sample	2
3	Simulated data samples	3
4	Boson jet identification	5
4.1	Jet reconstruction	5
4.2	Boson jet tagging	6
5	Event selection	8
5.1	Event topology	8
5.2	Boson tagging requirements	8
5.3	Dijet mass requirement	9
6	Background model	9
7	Systematic uncertainties	11
8	Results	14
8.1	Background fit to data	14
8.2	Statistical analysis	15
8.3	Exclusion limits on new diboson resonances	16
9	Conclusions	17
	The ATLAS collaboration	22

1 Introduction

The substantial dataset of Large Hadron Collider (LHC) proton-proton (pp) collisions at $\sqrt{s} = 8$ TeV collected by the ATLAS experiment provides a distinct opportunity to search for new heavy resonances at the TeV mass scale. This paper presents a search for narrow diboson resonances (WW , WZ and ZZ) decaying to fully hadronic final states. The fully hadronic mode has a higher branching fraction than leptonic and semileptonic decay modes, and is therefore used to extend the reach of the search to the highest possible resonance masses.

W and Z bosons resulting from the decay of very massive resonances are highly boosted, so that each boson's hadronic decay products are reconstructed as a single jet. The signature of the heavy resonance decay is thus a resonance structure in the dijet invariant mass spectrum. The dominant background for this search is due to dijet events from QCD processes, which produce a smoothly falling spectrum without resonance structures. To cope with this large background, jets are selected using a boson tagging procedure based on

a reclustering-mass-drop filter (BDRS-A, similar to the method introduced in ref. [1]), jet mass, and further substructure properties. The tagging procedure strongly suppresses the dijet background, although these QCD processes still overwhelm the expected backgrounds from single boson production with one or more jets, Standard Model (SM) diboson production, single-top and top-pair production. As all of these background sources produce dijet invariant mass distributions without resonance peaks, the expected background in the search is modelled by a fit to a smoothly falling distribution.

Diboson resonances are predicted in several extensions to the SM, such as technicolour [2–4], warped extra dimensions [5–7], and Grand Unified Theories [8–11]. To assess the sensitivity of the search, to optimise the event selection, and for comparison with data, two specific benchmark models are used: an extended gauge model (EGM) $W' \rightarrow WZ$ where the spin-1 W' gauge boson has a modified coupling to the SM W and Z bosons [12–14], and a spin-2 graviton, $G_{\text{RS}} \rightarrow WW$ or ZZ , a Kaluza-Klein mode [5, 15] of the bulk Randall-Sundrum (RS) graviton [16–18].

The CMS collaboration has performed a search for diboson resonances with the fully hadronic final state [19] of comparable sensitivity to the one presented in this article. In this search, the EGM $W' \rightarrow WZ$ with masses below 1.7 TeV and G_{RS} of the original RS model decaying to WW with masses below 1.2 TeV are excluded at 95% confidence level (CL). The CMS collaboration has also published upper limits on the production of generic diboson resonances using semileptonic final states [20]. Using the $\ell\ell q\bar{q}$ final state, the ATLAS collaboration has excluded at 95% CL a bulk $G_{\text{RS}} \rightarrow ZZ$ with mass below 740 GeV [21]. For narrow resonances decaying exclusively to WZ or WW , the sensitivity of the ATLAS search in the $\ell\nu q\bar{q}$ channel [22] is comparable to that of the search presented here in the mass range from 1.3 to 2.5 TeV. That search has also excluded a bulk $G_{\text{RS}} \rightarrow WW$ with mass below 760 GeV.

2 ATLAS detector and data sample

The ATLAS detector [23] surrounds nearly the entire solid angle around the ATLAS collision point. It has an approximately cylindrical geometry and consists of an inner tracking detector surrounded by electromagnetic and hadronic calorimeters and a muon spectrometer. The tracking detector is placed within a 2 T axial magnetic field provided by a superconducting solenoid and measures charged-particle trajectories with pixel and silicon microstrip detectors that cover the pseudorapidity¹ range $|\eta| < 2.5$, and with a straw-tube transition radiation tracker covering $|\eta| < 2.0$.

A high-granularity electromagnetic and hadronic calorimeter system measures the jets in this analysis. The electromagnetic calorimeter is a liquid-argon (LAr) sampling calorimeter with lead absorbers, spanning $|\eta| < 3.2$ with barrel and end-cap sections. The three-

¹ATLAS uses a right-handed coordinate system with its origin at the nominal interaction point (IP) in the centre of the detector and the z -axis along the beam pipe. The x -axis points from the IP to the centre of the LHC ring, and the y -axis points upward. Cylindrical coordinates (r, ϕ) are used in the transverse plane, ϕ being the azimuthal angle around the beam pipe. The pseudorapidity is defined in terms of the polar angle θ as $\eta = -\ln \tan(\theta/2)$.

layer central hadronic calorimeter comprises scintillator tiles with steel absorbers and extends to $|\eta| = 1.7$. The hadronic end-cap calorimeters measure particles in the region $1.5 < |\eta| < 3.2$ using liquid argon with copper absorber. The forward calorimeters cover $3.1 < |\eta| < 4.9$, using LAr/copper modules for electromagnetic energy measurements and LAr/tungsten modules to measure hadronic energy.

Events are recorded in ATLAS if they satisfy a three-level trigger requirement. The level-1 trigger detects jet and particle signatures in the calorimeter and muon systems with a fixed latency of $2.5 \mu\text{s}$, and is designed to reduce the event rate to less than 75 kHz. Jets are identified at level-1 with a sliding-window algorithm, searching for local maxima in square regions with size $\Delta\eta \times \Delta\phi = 0.8 \times 0.8$. The subsequent high-level trigger consists of two stages of software-based trigger filters which reduce the event rate to a few hundred Hz. Events used in this search satisfy a single-jet trigger requirement, based on at least one jet reconstructed at each trigger level. At the first filtering stage of the high-level trigger, jet candidates are reconstructed from calorimeter cells using a cone algorithm with small radius, $R = 0.4$. The final filter in the high-level trigger requires a jet to satisfy a higher transverse momentum (p_T) threshold, reconstructed with the anti- k_t algorithm [24] and a large radius parameter ($R = 1.0$).

This search is performed using the dataset collected in 2012 from 8 TeV LHC pp collisions using a single-jet trigger with a nominal p_T threshold of 360 GeV. The integrated luminosity of this dataset after requiring good beam and detector conditions is 20.3 fb^{-1} , with a relative uncertainty of $\pm 2.8\%$. The uncertainty is derived following the methodology detailed in ref. [25].

3 Simulated data samples

The leading-order Monte Carlo (MC) generator PYTHIA 8.170 [26] is used to model $W' \rightarrow WZ$ events in order to determine and optimise the sensitivity of this search. PYTHIA 8 uses the p_T -ordered showering introduced in PYTHIA 6.3 [27, 28], and interleaves multiple parton interactions with both initial- and final-state radiation. The samples generated for this analysis use MSTW2008 [29] parton distribution functions (PDFs), with parton shower parameters tuned to ATLAS underlying-event data [30]. Hadronisation is based on the Lund string fragmentation framework [31]. An additional set of W' samples generated with PYTHIA for the hard scattering interaction and HERWIG++ [32] for parton showering and hadronisation is used to assess systematic uncertainties on the signal efficiency due to uncertainties on the parton shower and hadronisation model. These samples use angular-ordered showering and cluster hadronisation.

The W' boson samples are generated for different resonance masses, covering the range $1.3 \leq m_{W'} \leq 3.0 \text{ TeV}$ in 100 GeV intervals. The W' is required to decay to a W and a Z boson, which are both forced to decay hadronically. The cross section times branching ratio as well as the resonance width for the samples listed in table 1 are calculated by PYTHIA 8 assuming EGM couplings [12] for the W' . In particular, the W' coupling to WZ is equal to that of the W coupling scaled by $c \times (m_W/m_{W'})^2$, where c is a coupling scaling factor of order one which is set to unity for the samples generated here. The partial

m [TeV]	$\Gamma_{W'}$ [GeV]	$\Gamma_{G_{RS}}$ [GeV]	$W' \rightarrow WZ$		$G_{RS} \rightarrow WW$		$G_{RS} \rightarrow ZZ$	
			$\sigma \times \text{BR}$ [fb]	$f_{10\%}$	$\sigma \times \text{BR}$ [fb]	$f_{10\%}$	$\sigma \times \text{BR}$ [fb]	$f_{10\%}$
1.3	47	76	19.1	0.83	0.73	0.85	0.37	0.84
1.6	58	96	6.04	0.79	0.14	0.83	0.071	0.84
2.0	72	123	1.50	0.72	0.022	0.83	0.010	0.82
2.5	91	155	0.31	0.54	0.0025	0.78	0.0011	0.78
3.0	109	187	0.088	0.31	0.00034	0.72	0.00017	0.71

Table 1. The resonance width (Γ) and the product of cross sections and branching ratios (BR) to four-quark final states used in modelling $W' \rightarrow WZ$, $G_{RS} \rightarrow WW$, and $G_{RS} \rightarrow ZZ$, for several values of resonance pole masses (m). The fraction of events in which the invariant mass of the W' or G_{RS} decay products lies within 10% of the nominal resonance mass ($f_{10\%}$) is also displayed.

width of $W' \rightarrow WZ$ decays thus scales linearly with $m_{W'}$, leading to a narrow width over the entire accessible mass range. Because of the anti-quark parton distribution functions involved in the production, a significant part of the W' cross section for large W' masses is due to off-shell interactions which produce a low-mass tail in the W' mass spectrum. The relative size of the low-mass tail increases with the W' mass: the fraction of events with a diboson mass below 20% of the pole mass of the W' increases from 10% for $m_{W'} = 1.3$ TeV to 22% for $m_{W'} = 2.0$ TeV and to 65% for $m_{W'} = 3.0$ TeV.

An extended RS model with a warped extra dimension is used for the excited graviton benchmarks. In this model the SM fields are allowed to propagate in the warped extra dimension [16], avoiding the constraints on the original RS model from limits on flavour-changing neutral currents and electroweak precision measurements. The model is characterised by a dimensionless coupling constant $k/\bar{M}_{\text{Pl}} \sim 1$, where k is the curvature of the warped extra dimension and \bar{M}_{Pl} is the reduced Planck mass. The RS excited graviton samples are generated with CalcHEP 3.4 [33] setting $k/\bar{M}_{\text{Pl}} = 1$, covering the resonance mass range $1.3 \leq m_{G_{RS}} \leq 3.0$ TeV in 100 GeV intervals. The graviton resonance is decayed to WW or ZZ , and the resulting W or Z bosons are forced to decay hadronically. The cross section times branching ratio as well as the resonance width calculated by CalcHEP for the RS model are listed in table 1. Events are generated using CTEQ6L1 [34] PDFs, and use PYTHIA 8 for the parton shower and hadronisation.

To characterise the expected dijet invariant mass spectrum in the mass range 1.3–3.0 TeV, simulated QCD dijet events, diboson events, and single W or Z bosons produced with jets are used. Contributions from SM diboson events are expected to account for approximately 6% of the selected sample, and single boson production is expected to contribute less than 2%. Contributions from $t\bar{t}$ production, studied using MC@NLO [35] and HERWIG [36] showering, were found to be negligible and are not considered further.

QCD dijet events are produced with PYTHIA 8 and the CT10 [37] PDFs and the W/Z + jets samples are produced with PYTHIA 8 and CTEQ6L1 PDFs. Diboson events are produced at the generator level with POWHEG [38], using PYTHIA for the soft parton shower. The samples of single W or Z bosons produced with jets are further used to determine a scale factor for the efficiency of the boson tagging selection, by comparing the

boson tagging efficiencies between simulation and collision data in a W/Z +jets-enriched sample.

The final-state particles produced by the generators are propagated through a detailed detector simulation [39] based on GEANT4 [40]. The average number of pp interactions per bunch crossing was approximately 20 while the collision data were collected. The expected contribution from these additional minimum-bias pp interactions is accounted for by overlaying additional minimum-bias events generated with PYTHIA 8, matching the distribution of the number of interactions per bunch crossing observed in collision data. Simulated events are then reconstructed with the same algorithms run on collision data.

4 Boson jet identification

In this search W and Z bosons from the decay of the massive resonance are produced with a large transverse momentum relative to their mass and each boson is reconstructed as a single large-radius jet. Boson jet-candidates are then identified by applying tagging requirements based on the reconstructed jet properties, as described below.

4.1 Jet reconstruction

Jets are formed by combining topological clusters [41] reconstructed in the calorimeter system, which are calibrated in energy with the local calibration scheme [42] and are considered massless. These topological clusters are combined into jets using the Cambridge-Aachen (C/A) algorithm [43, 44] implemented in FastJet [45] with a radius parameter $R = 1.2$. The C/A algorithm iteratively replaces the nearest pair of elements (topological clusters or their combination) with their combination² until all remaining pairs are separated by more than R , defining the distance ΔR between elements as $(\Delta R)^2 = (\Delta y)^2 + (\Delta\phi)^2$ where y is the rapidity. The jets are the elements remaining after this final stage of iteration, and the last pair of elements to be combined into a given jet are referred to here as the subjets of that jet. Charged-particle tracks reconstructed in the tracking detector are matched to these calorimeter jets if they fall within the passive catchment area of the jet [46], determined by representing each track by a collinear “ghost” constituent with negligible energy during jet reconstruction. Only well-reconstructed tracks with $p_T \geq 500$ MeV and consistent with particles originating at the primary³ collision vertex are considered.

The jets are then groomed to identify the pair of subjets associated with the $W \rightarrow q\bar{q}'$ or $Z \rightarrow q\bar{q}$ decay, and to reduce the effect of pileup and other noise sources on the resolution. The grooming algorithm is a variant of the mass-drop filtering technique [1], which first examines the sequence of pairwise combinations used to reconstruct the jet in reverse order. At each step the lower-mass subjet is discarded, and the higher-mass subjet is considered as the jet, continuing until a pair is found which satisfies *mass-drop* and *subjet momentum balance* criteria parameterised by μ_f and $\sqrt{y_f}$, respectively. Iteration stops when a pair of

²Elements are combined by summing their four-momenta.

³The primary collision vertex is the reconstructed vertex with the greatest sum of associated track p_T^2 .

Filtering parameter	Value
$\sqrt{y_f}$	0.2
μ_f	1
R_r	0.3
n_r	3

Table 2. Parameters for the mass-drop filtering algorithm used to groom C/A jets. The choice of μ_f parameter corresponds to no mass-drop requirement being imposed in the grooming procedure.

subjects is found for which each subjet mass $m_{(i)}$ satisfies $\mu \equiv m_{(i)}/m_0 \leq \mu_f$, and for which

$$\sqrt{y} \equiv \min(p_{Tj_1}, p_{Tj_2}) \frac{\Delta R_{(j_1, j_2)}}{m_0} \geq \sqrt{y_f},$$

where p_{Tj_1} and p_{Tj_2} are the transverse momenta of subjets j_1 and j_2 respectively, $\Delta R_{(j_1, j_2)}$ is the distance between subjets j_1 and j_2 , and m_0 is the mass of the parent jet.

The subjet momentum-balance threshold y_f and the mass-drop parameter μ_f used in this analysis, given in table 2, are chosen to stop the iteration when the two subjets corresponding to the W or Z boson decay have been identified in simulated signal events. The best signal to background ratio for a given signal efficiency was obtained with μ_f set to 1, hence no mass-drop requirement is applied in this analysis.

The selected pair of subjets is then filtered: the original topological cluster constituents of that pair of subjets are taken together and clustered using the C/A algorithm with a small radius parameter ($R_r = 0.3$), and all but the three ($n_r = 3$) highest- p_T jets resulting from this reclustering of the subjets' constituents are discarded. If there are fewer than three jets after the reclustering, all constituents are kept. Those constituents that remain form the resulting filtered jet, which is further calibrated using energy- and η -dependent correction factors derived from simulation by applying a procedure similar to the one used in ref. [47]. The calibrated four-momentum is used as the W or Z boson candidate's four-momentum in subsequent cuts and in reconstructing the heavy resonance candidate's mass in each selected event.

4.2 Boson jet tagging

The grooming algorithm rejects jets that do not satisfy the momentum balance and mass-drop criteria at any stage of iteration, and thus provides a small degree of discriminating power between jets from hadronically decaying bosons and those from QCD dijet production. To improve the discrimination in this analysis, the remaining jets are also tagged with three additional boson tagging requirements. First, a more stringent subjet momentum-balance criterion ($\sqrt{y} \geq 0.45$) is applied to the pair of subjets identified by the filtering algorithm at the stopping point before the reclustering stage, since jets in QCD dijet events that survive grooming tend to have unbalanced subjet momenta characteristic of soft gluon radiation. Figure 1a shows the subjet momentum-balance distribution for jets in signal and QCD dijet background simulated events. Unlike jets from massive boson decays in which the hadron multiplicity is essentially independent of the jet p_T , energetic gluon jets are

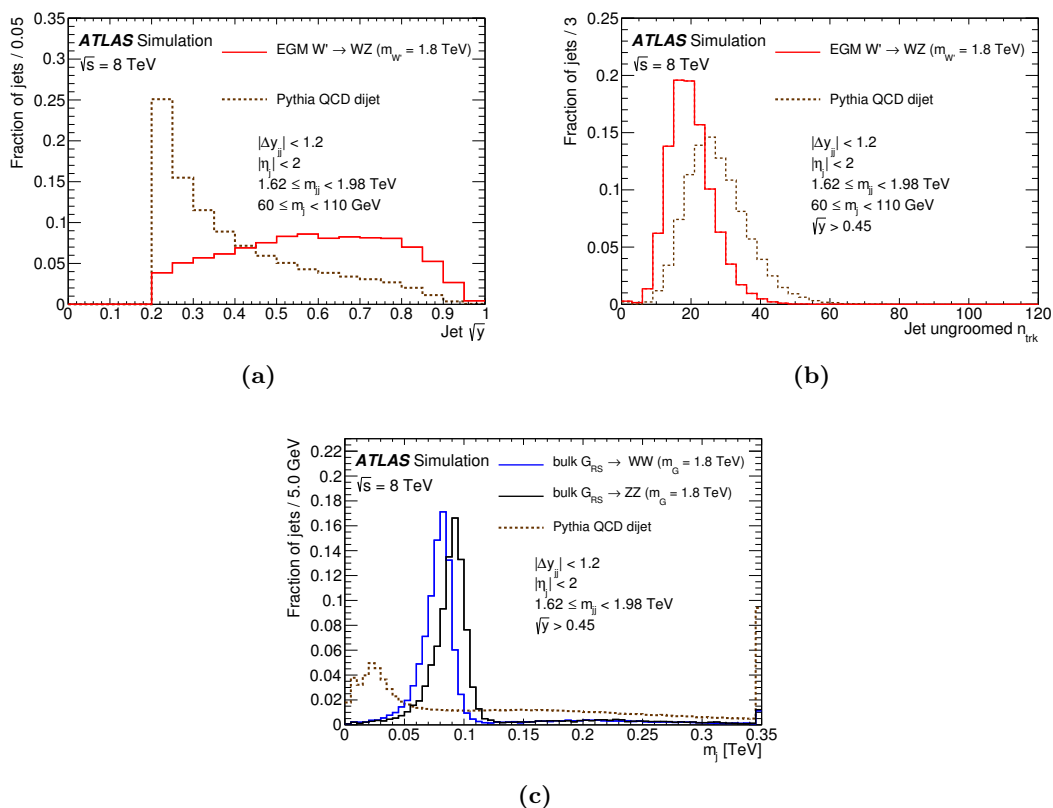


Figure 1. The distribution of the boson-tagging variables (a) subjet momentum balance \sqrt{y} , (b) number of tracks n_{trk} matched to the jet, and (c) mass m_j of the groomed jet, in simulated signal and background events. The signal and background distributions are normalised to unit area, and the last bin of each histogram includes the fraction of events falling outside of the displayed range. Requirements are placed on the events used to ensure that the kinematics of the signal and background events are comparable.

typically composed of more hadrons, so the number of charged-particle tracks associated with the original, ungroomed jet is required to be small ($n_{\text{trk}} < 30$). Figure 1b shows the number of tracks matched to jets for selected jets in signal and background simulated events. The efficiency of this selection requirement must be corrected by a scale factor derived from data, as explained in section 7. Finally, a selection window is applied to the invariant mass of the filtered jet, m_j , since this quantity is expected to be small for jets in QCD dijet events and to reflect the boson mass for jets from hadronic boson decays. The expected mass distribution of jets in G_{RS} simulated events and the dijet background simulation is illustrated in figure 1c. Narrow mass windows with a width of 26 GeV are chosen to optimise sensitivity to signal events and are centred at either 82.4 GeV or 92.8 GeV, where the mass distributions of the W and Z jets, respectively, peak in simulation. Each jet’s mass must fall within either the W or Z mass window, consistent with the WZ , WW or ZZ final state being studied.

5 Event selection

High-mass resonances decaying to a pair of boosted vector bosons with subsequent hadronic decay are recognised as two large-radius massive jets with large momentum, typically balanced in p_T . Events in this search must therefore first satisfy the high- p_T large-radius jet trigger, which is found to select over 99% of C/A $R=1.2$ jets within $|\eta| < 2.0$ and with ungroomed p_T greater than 540 GeV. Events are removed if they contain a prompt electron candidate with $E_T > 20$ GeV in the regions $|\eta| < 1.37$ or $1.52 < |\eta| < 2.47$, or a prompt muon candidate with $p_T > 20$ GeV in the region $|\eta| < 2.5$. This requirement ensures that this analysis has no events in common with other diboson search analyses [21, 22]. Events with reconstructed missing transverse momentum exceeding 350 GeV are also removed, as these are used in searches sensitive to diboson resonances with a Z boson decaying to neutrinos [48].

5.1 Event topology

For events satisfying the requirements above, two C/A $R=1.2$ jets with p_T exceeding 20 GeV must be found and must pass the mass-drop filtering procedure. The two jets with the highest transverse momentum must have $|\eta| < 2.0$ to ensure sufficient overlap with the inner tracking detector, since associated charged-particle tracks are used in the boson tagging requirements and for estimating systematic uncertainties. In addition, a requirement on the rapidity difference between the two leading jets, $|y_1 - y_2| < 1.2$, is imposed to improve the sensitivity. This rapidity difference is smaller for s -channel processes such as the W' and G_{RS} signal models than for the t -channel processes dominating the QCD dijet background.

The combined efficiency of these three cuts in W' signal events is between 72% and 81% depending on the resonance mass, for events from each signal sample in which the true diboson mass lies within 10% of the nominal value. For G_{RS} signal events, the combined efficiency is between 82% and 87%. The difference in the expected efficiencies between the W' and G_{RS} signals is related to the different event topologies expected for spin-1 and spin-2 resonances affecting acceptance.

A selection on the p_T asymmetry of the two leading jets, $(p_{T1} - p_{T2}) / (p_{T1} + p_{T2}) < 0.15$, is used to reject events where one of the jets is poorly measured or does not come from the primary pp collision. The signal selection efficiency of this cut exceeds 97% in W' signal samples and 90% in the samples of G_{RS} events. The difference in the expected efficiencies between the W' and G_{RS} signals is related to their different production mechanisms. Figure 2a shows the selection efficiency of the event topology requirements for signal events with resonance mass within 10% of the nominal signal mass for the $W' \rightarrow WZ$, bulk $G_{RS} \rightarrow WW$ and bulk $G_{RS} \rightarrow ZZ$ benchmark models, with statistical and systematic uncertainties indicated by the width of the bands in the figure.

5.2 Boson tagging requirements

The two jets with the highest transverse momentum each must satisfy the three boson tagging requirements discussed in section 4: $\sqrt{y} \geq 0.45$, $n_{\text{trk}} < 30$, and $|m_j - m_V| < 13$ GeV, where m_V is the peak value of the reconstructed W or Z boson mass distribution. For the

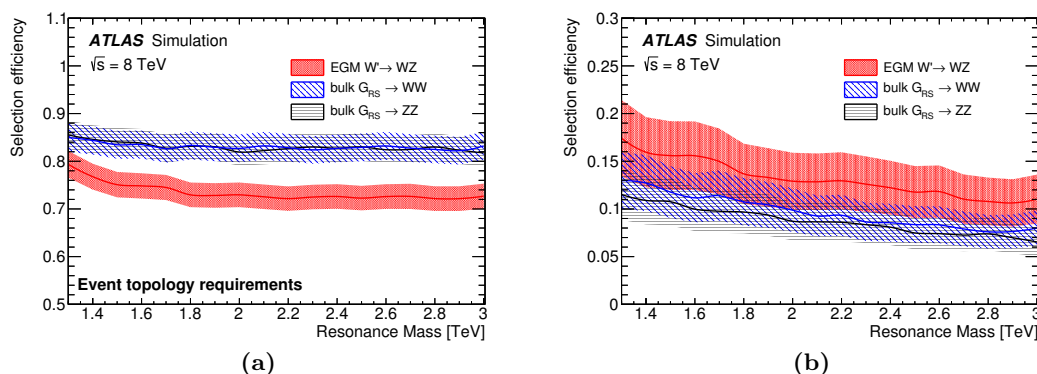


Figure 2. Event selection efficiencies as a function of the resonance masses for EGM $W' \rightarrow WZ$ and bulk $G_{RS} \rightarrow WW$ and ZZ for simulated events with resonance mass within 10% of the nominal signal mass. In (a), the event topology requirements are applied to EGM $W' \rightarrow WZ$, $G_{RS} \rightarrow WW$ and $G_{RS} \rightarrow ZZ$ samples, while in (b), the WZ , WW and ZZ boson tagging selections are also applied in the EGM $W' \rightarrow WZ$, $G_{RS} \rightarrow WW$ and $G_{RS} \rightarrow ZZ$ samples respectively and the efficiencies shown are corrected by the simulation-to-data scale factor. The width of the bands in each figure indicates both the statistical and systematic uncertainties.

$W' \rightarrow WZ$ search, this final cut sets m_V equal to the peak reconstructed W boson mass when applied to the lower mass jet, and to the peak reconstructed Z boson mass when applied to the higher mass jet.

The expected efficiency of these boson tagging cuts applied to signal events is evaluated using the MC signal samples described in section 3. For signal events passing event topology requirements on the mass-drop filtering, η , the rapidity difference, and the p_T asymmetry, the average efficiency of the tagging cuts for each of the two leading- p_T filtered jets is approximately the same in the $G_{RS} \rightarrow WW$ and $G_{RS} \rightarrow ZZ$ samples, and ranges from 44.0% in the $m_{G_{RS}} = 1.2$ TeV sample to 33.9% for the $m_{G_{RS}} = 3.0$ TeV sample. Figure 2b shows the selection efficiency of the event selection and tagging requirements for signal events with resonance mass within 10% of the nominal signal mass for the $W' \rightarrow WZ$ and bulk $G_{RS} \rightarrow WW$ and bulk $G_{RS} \rightarrow ZZ$ benchmark models, with both statistical and systematic uncertainties included in the error band. The average background selection efficiency of the tagger for each of the two leading- p_T filtered jets in simulated QCD dijet events satisfying the same event selection requirements ranges from 1.2% for events with dijet masses between 1.08 TeV and 1.32 TeV, to 0.6% for events with dijet masses between 2.7 TeV and 3.3 TeV.

5.3 Dijet mass requirement

The invariant mass calculated from the two leading jets must exceed 1.05 TeV. This requirement restricts the analysis of the dijet mass distribution to regions where the trigger is fully efficient for boson-tagged jets, so that the trigger efficiency does not affect its shape.

6 Background model

The search for high-mass diboson resonances is carried out by looking for resonance structures on a smoothly falling dijet invariant mass spectrum, empirically characterised by the

function

$$\frac{dn}{dx} = p_1(1-x)^{p_2+\xi p_3} x^{p_3}, \quad (6.1)$$

where $x = m_{jj}/\sqrt{s}$, and m_{jj} is the dijet invariant mass, p_1 is a normalisation factor, p_2 and p_3 are dimensionless shape parameters, and ξ is a dimensionless constant chosen after fitting to minimise the correlations between p_2 and p_3 . A maximum-likelihood fit, with parameters p_1 , p_2 and p_3 free to float, is performed in the range $1.05 \text{ TeV} < m_{jj} < 3.55 \text{ TeV}$, where the lower limit is dictated by the point where the trigger is fully efficient for tagged jets and the upper limit is set to be in a region where the data and the background estimated by the fit are well below one event per bin for the tagged distributions. The likelihood is defined in terms of events binned in 100-GeV-wide bins in m_{jj} as

$$\mathcal{L} = \prod_i \frac{\lambda_i^{n_i} e^{-\lambda_i}}{n_i!}, \quad (6.2)$$

where n_i is the number of events observed in the i^{th} m_{jj} bin and λ_i is the background expectation for the same bin.

The functional form in eq. (6.1) is tested for compatibility with distributions similar to the expected background by applying it to simulated background events and to several sidebands in the data. Figure 3 shows fits to the HERWIG++ and PYTHIA simulated dijet events that pass the full event selection and tagging requirements on both jets, where the predictions from these leading-order generators are corrected by reweighting the untagged leading-jet p_T distributions to match the untagged distribution in data. Figure 4 shows the results of fitting the dijet mass spectrum before tagging, and in otherwise tagged events where both the leading and subleading jet have masses falling below the boson-tagging mass windows, in the range $40 < m_j < 60 \text{ GeV}$. For the data selected before boson tagging, the trigger efficiency as a function of the dijet mass is taken into account in the fit, because in the untagged jet sample the trigger is not fully efficient in the first dijet mass bin displayed. The fitted background functions in figures 3 and 4 are integrated over the same bins used to display the data, and labelled “background model” in the figures. The size of the shaded band reflects the uncertainties of the fit parameters. In figure 4a the background model is shown, but the size of the uncertainty band is too small to be seen. The lower insets in the figures show the significance, defined as the signed z -value of the difference between the distribution being modelled and the background model’s prediction [49]. The significance with respect to the maximum-likelihood expectation is displayed in red, and the significance when taking the uncertainties on the fit parameters into account is shown in blue.

Table 3 summarises the results of these fits, as well as fits to data where one jet mass falls in the low-mass sideband ($40 < m_j \leq 60 \text{ GeV}$) and the other falls in a high-mass sideband from $110 < m_j < 140 \text{ GeV}$, and where both jet masses fall in the high-mass sideband. The dijet mass distribution of the simulated background and of each of these background-dominated selections are well-described by the functional form in eq. (6.1).

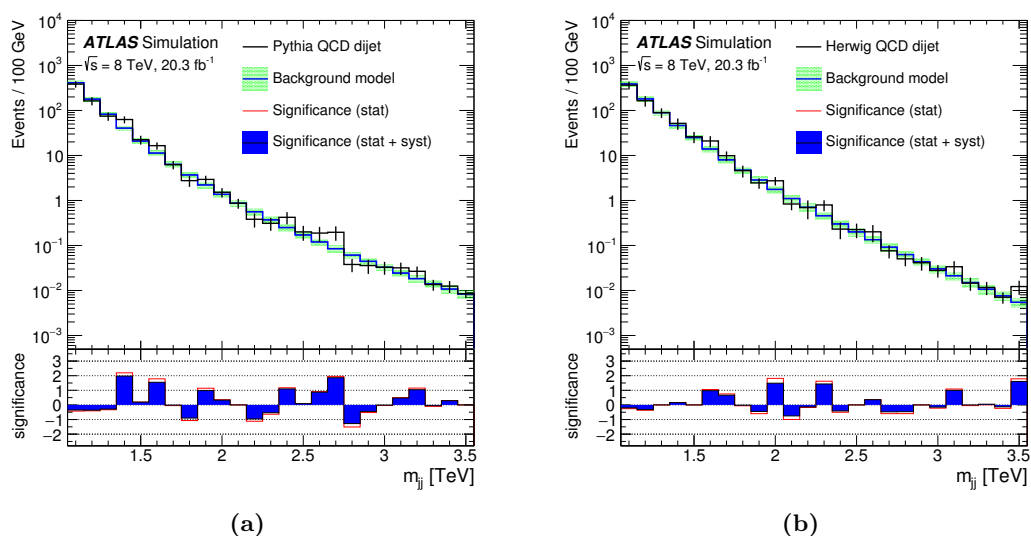


Figure 3. Fits of the background model to the dijet mass (m_{jj}) distributions in (a) PYTHIA 8 and (b) HERWIG++ simulated background events that have passed all event selection and tagging requirements. The events are reweighted in both cases to correctly reproduce the leading-jet p_T distribution for untagged events, and the simulated data samples were scaled to correspond to a luminosity of 20.3 fb^{-1} . The significance shown in the inset for each bin is calculated using the statistical errors of the simulated data.

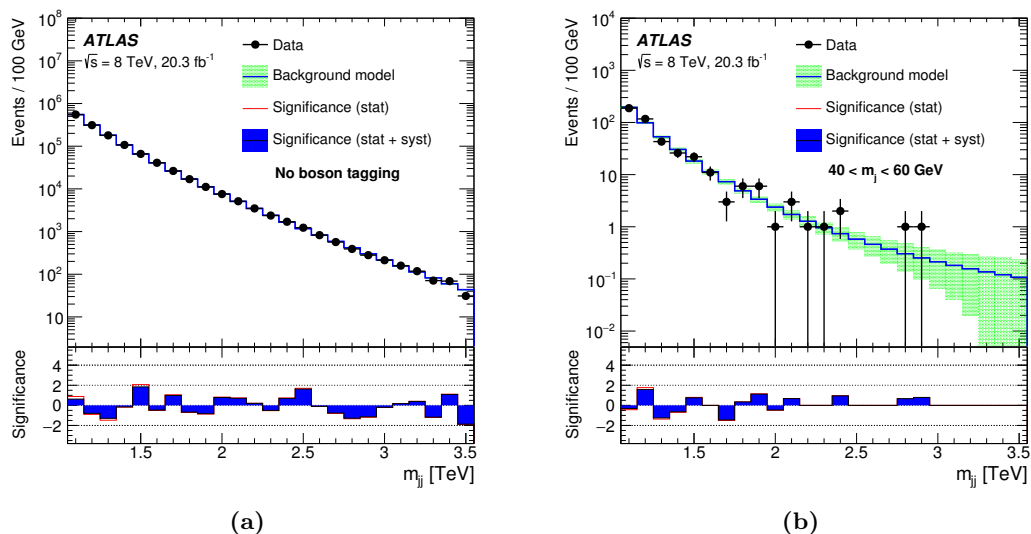


Figure 4. Fits of the background model to the dijet mass (m_{jj}) distributions in data events (a) before boson tagging, and (b) where both jets pass all tagging requirements except for the m_j requirement, and instead satisfy $40 < m_j \leq 60 \text{ GeV}$.

7 Systematic uncertainties

The uncertainty on the background expectation is determined by the fitting procedure, which assumes a smoothly falling m_{jj} distribution. Possible uncertainties due to the back-

Sample	χ^2/nDOF	Probability
PYTHIA dijet events	24.6/22	0.31
HERWIG++ dijet events	15.9/22	0.82
Data with $110 < m_{j1} \leq 140$ GeV and $40 < m_{j2} \leq 60$ GeV	12.1/11	0.79
Data with $40 < m_j \leq 60$ GeV for both jets	19.8/13	0.56
Data with $110 < m_j \leq 140$ GeV for both jets	5.0/6	0.91

Table 3. Goodness-of-fit for maximum-likelihood fits of the background model to the dijet mass distribution in simulated events, and in selected mass sidebands from data events where at least one of the leading and subleading jet fails the jet mass selection. One-sided χ^2 probabilities are displayed; for the three data sideband fits, these probabilities were calibrated using pseudo-experiments to avoid biases due to empty bins.

ground model were assessed by investigating several alternative families of parametrisations, and by considering signal plus background fits of the chosen function to simulations of the dominant background as well as sidebands and control regions of data in which a signal contribution is expected to be negligible. These effects were estimated to be no more than 25% of the statistical uncertainty at any mass in the search region. The effect of the uncertainty on the trigger efficiency, the variations of the selection efficiencies as a function of the kinematic properties of the background, and the composition of the background were also studied and were found to be well-covered by the uncertainties from the fit.

Systematic uncertainties on the shape of the m_{jj} distribution and the normalisation of the W' and G_{RS} signal are expressed as nuisance parameters with specified probability distribution functions (pdfs). The overall normalisation is a product of scale factors, each corresponding to an identified nuisance parameter. If the shape is affected by a given nuisance parameter, the systematic change is included when the signal distribution is generated. If the nuisance parameter does not affect the shape, but only affects the normalisation, the distribution is simply scaled.

The jet p_T scale α_{p_T} is defined as a multiplicative factor to the jet p_T in simulation, $p_T = \alpha_{p_T} p_T^{\text{MC}}$. Following the technique used in ref. [47], the systematic uncertainty on α_{p_T} is assessed by applying the jet reconstruction and filtering algorithms to inner-detector track constituents, which are treated as massless, and matching these track jets to the calorimeter jets. The ratio of the matched track jet's p_T to the calorimeter jet's p_T as a function of several kinematic variables is compared in simulation and data and found to be consistent within 2%. Hence, the pdf used for α_{p_T} is a Gaussian with a mean of one and a standard deviation of 0.02. Similar methods are used to determine the pdfs for the scale uncertainties in jet mass m_j and momentum balance \sqrt{y} .

Mismodelling the jet p_T resolution can change the reconstructed width of a diboson resonance. The jet p_T resolution in the simulation is 5% in this kinematic region, and a 20% systematic uncertainty on this resolution is implemented by applying a multiplicative smearing factor, r_E , to the p_T of each reconstructed jet with a mean value of unity and a width $|\sigma_{r_E}|$. The nuisance parameter σ_{r_E} represents the uncertainty in the p_T resolution

Source	Uncertainty	Constraining pdf
Jet p_T scale	2%	$G(\alpha_{p_T} 1, 0.02)$
Jet p_T resolution	20%	$G(\sigma_{r_E} 0, 0.05 \times \sqrt{1.2^2 - 1^2})$
Jet mass scale	3%	$G(\alpha_m 1, 0.03)$

Table 4. Summary of the systematic uncertainties affecting the shape of the signal dijet mass distribution and their corresponding models. $G(x|\mu, \sigma)$ in the table denotes a Gaussian distribution for the variable x with mean μ and standard deviation σ .

of reconstructed jets and is assumed to have a Gaussian pdf with a mean of zero and a standard deviation $0.05 \times \sqrt{1.2^2 - 1^2}$.

The pdfs for the uncertainties in jet-mass resolution and momentum-balance resolution, listed in table 4, are similarly constructed.

The n_{trk} variable is not modelled sufficiently well in simulation [50], so it is necessary to apply a scale factor to the simulated signal to correct the selection efficiency of the n_{trk} requirement. A scale factor of 0.90 ± 0.08 is derived from the ratio of the selection efficiency of this cut in a data control region enriched with $W/Z + \text{jets}$ events, where a high- p_T W or Z boson decays hadronically, to the selection efficiency of this cut in simulation. The data control region is defined by selecting events in the kinematic range where the jet trigger used in the search is fully efficient, and where only the leading- p_T jet passes the tagging requirement on \sqrt{y} . Fits to the jet mass spectrum of the leading- p_T jet determine the number of hadronically decaying W and Z bosons reconstructed as a single jet that pass the n_{trk} requirement as a function of the selection criteria on n_{trk} . The dominant uncertainty on these yields is the mismodelling of the jet mass spectrum for non- W or non- Z jets, and is evaluated by comparing the yields obtained when using two different background models in the fit. The resulting scale factor is 0.90 ± 0.08 . Since the n_{trk} requirement is applied twice per event in the selections used in the search, a scale factor of 0.8 is applied per selected signal event, with an associated uncertainty of 20%.

A 5% uncertainty on the signal efficiency due to uncertainties on the parton shower and hadronisation model is also included. The uncertainty is estimated by comparing the selection efficiencies obtained in simulated signal samples generated and showered with PYTHIA 8 to the selection efficiencies obtained in samples generated with PYTHIA 8 and showered with HERWIG++. An additional 3.5% uncertainty on the signal acceptance due to uncertainties on the PDFs is considered. This uncertainty is estimated according to the PDF4LHC recommendations [51].

Table 4 summarises the systematic uncertainties affecting the signal shape and the pdf constraining the associated nuisance parameter. The largest uncertainty on the shape of the reconstructed signal is due to the jet p_T scale and resolution; the uncertainty in the scale introduces an uncertainty on the scale of the mass of the reconstructed resonant signal, and the resolution introduces an uncertainty of the width. The jet mass scale uncertainty also has an effect on the scale of the reconstructed mass, but this effect is less significant. Table 5 summarises the systematic uncertainties affecting the signal normalisation. The jet mass scale uncertainty affects both the shape and the normalisation.

Source	Normalisation uncertainty
Efficiency of the track-multiplicity cut	20.0%
Jet mass scale	5.0%
Jet mass resolution	5.5%
Subjet momentum-balance scale	3.5%
Subjet momentum-balance resolution	2.0%
Parton shower model	5.0%
Parton distribution functions	3.5%
Luminosity	2.8%

Table 5. Summary of the systematic uncertainties affecting the signal normalisation and their impact on the signal.

Parameter	Before tagging	WZ	WW	ZZ
ξ	4.3	3.8	4.2	4.5
p_2	30.95 ± 0.03	31.0 ± 1.4	32.5 ± 1.5	39.5 ± 2.0
p_3	-5.54 ± 0.03	-9.1 ± 1.5	-9.4 ± 1.6	-9.5 ± 2.3
Observed events	1335762	604	425	333

Table 6. Number of observed events and parameters from the background-only fits to the dijet mass spectrum for each tagging selection. The parameter ξ is a constant chosen after the fit to minimise the correlation between the fitted parameters p_2 and p_3 .

8 Results

8.1 Background fit to data

The fitting procedure is applied to the data after WZ , WW and ZZ selection, and the results are shown in figure 5. In this figure, the fitted background functions, labelled “background model”, are again integrated over the same bins used to display the data, and the size of the shaded band reflects the uncertainties on the parameters propagated to show the uncertainty on the expectation from the fit. Figure 5 also displays the fitted dijet mass distribution of events passing any of the three tagging selections. The lower panels in the figure show the significance of the difference between data and the expectation in each bin. Table 6 gives the fitted values of the parameters for the data selected before tagging, displayed in figure 4a, and after the WZ , WW and ZZ selections, as well as the number of events observed.

The dijet mass distributions after all three tagging selections are well-described by the background model over the entire mass range explored, with the exception of a few bins near $m_{jj} = 2$ TeV which contain more events than predicted by the background model. Approximately 20% of the events selected by either the WW , WZ , or ZZ selection are shared among all three signal regions. The fraction of events common to the WZ and the WW or the WZ and the ZZ selections are 49% and 43% respectively. After requiring that $m_{jj} > 1.75$ TeV, 5 out of 25 events are common to all three signal regions. The statistical interpretation of these dijet mass distributions is discussed in the following section.

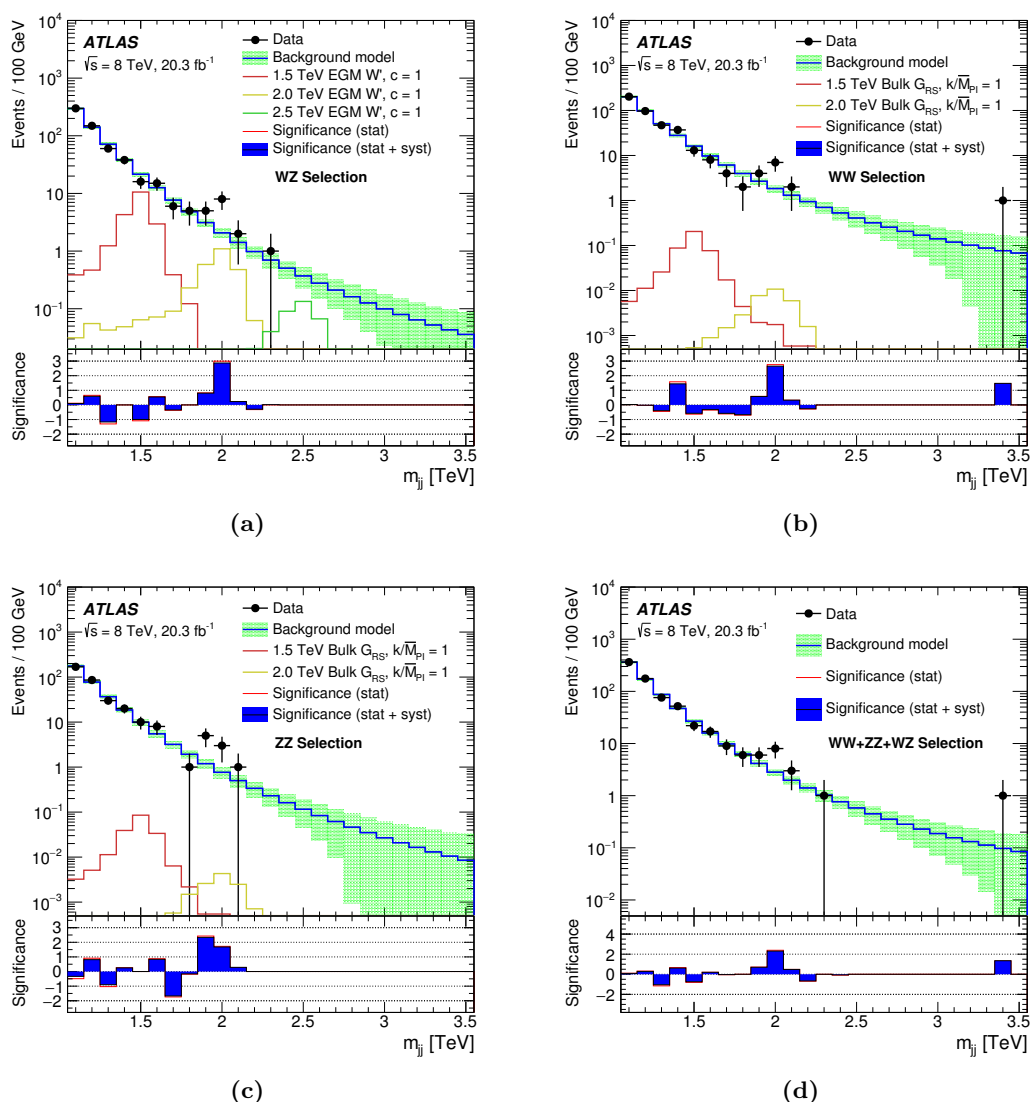


Figure 5. Background-only fits to the dijet mass (m_{jj}) distributions in data (a) after tagging with the WZ selection, (b) after tagging with the WW selection, (c) after tagging with the ZZ selection, and (d) for events passing any of the three tagging selections. The significance shown in the inset for each bin is the difference between the data and the fit in units of the uncertainty on this difference. The significance with respect to the maximum-likelihood expectation is displayed in red, and the significance when taking the uncertainties on the fit parameters into account is shown in blue. The spectra in the three signal regions are compared to the signals expected for an EGM W' with $m_{W'} = 1.5, 2.0,$ or 2.5 TeV or to an RS graviton with $m_{G_{RS}} = 1.5$ or 2.0 TeV.

8.2 Statistical analysis

A frequentist analysis is used to interpret the data. For each of the two benchmark models under test, the parameter of interest in the statistical analysis is the signal strength, μ , defined as a scale factor on the total number of signal events predicted by the model. Thus, the background-only hypothesis corresponds to $\mu = 0$, and the hypothesis of a

signal-plus-background model corresponds to $\mu = 1$. A test statistic, $\lambda(\mu)$, based on the profile likelihood ratio [52] is used to test these models. The test statistic is designed to extract the information on μ from a maximum-likelihood fit of the signal-plus-background model to the data.

The likelihood model for the observation is

$$\mathcal{L} = \prod_i P_{\text{pois}}(n_{\text{obs}}^i | n_{\text{exp}}^i) \times G(\alpha_{\text{PT}}) \times G(\alpha_{\text{m}}) \times G(\sigma_{r_{\text{E}}}) \times \mathcal{N}(\theta) \quad (8.1)$$

where $P_{\text{pois}}(n_{\text{obs}}^i | n_{\text{exp}}^i)$ is the Poisson probability to observe n_{obs}^i events if n_{exp}^i events are expected, $G(\alpha_{\text{PT}})$, $G(\alpha_{\text{m}})$, and $G(\sigma_{r_{\text{E}}})$, are the pdfs of the nuisance parameters modelling the systematic uncertainties related to the shape of the signal, and \mathcal{N} is a log-normal distribution for the nuisance parameters, θ , modelling the systematic uncertainty on the signal normalisation. The expected number of events is the bin-wise sum of the events expected for the signal and background: $\mathbf{n}_{\text{exp}} = \mathbf{n}_{\text{sig}} + \mathbf{n}_{\text{bg}}$. The number of expected background events in dijet mass bin i , n_{bg}^i , is obtained by integrating dn/dx obtained from eq. (6.1) over that bin. Thus \mathbf{n}_{bg} is a function of the dijet background parameters p_1, p_2, p_3 . The number of expected signal events, \mathbf{n}_{sig} , is evaluated based on MC simulation assuming the cross section of the model under test multiplied by the signal strength and including the effects of the systematic uncertainties described in section 7. The expected number of signal events is a function of μ and the nuisance parameters modelling the systematic uncertainties on the signal.

The compatibility of the data with the background-only expectation is quantified in terms of the local p_0 , defined as the probability of the background-only model to produce an excess at least as large as the one observed and quantified with an ensemble of 500,000 background-only pseudo-experiments, while the global probability of an excess with a given local p_0 being the most significant excess to be observed anywhere in the search region is quantified with 100,000 background-only pseudo-experiments that take into account the mass ranges and overlapping event samples for the three channels. The largest discrepancies, in the region around 2 TeV in figures 5a, 5b and 5c, lead to small p_0 values near that mass. The smallest local p_0 values in the WZ , WW , and ZZ channels correspond to significances of 3.4σ , 2.6σ , and 2.9σ respectively. Considering the entire mass range of the search (1.3–3.0 TeV) in each of the three search channels, the global significance of the discrepancy in the WZ channel is 2.5σ .

Exclusion limits at the 95% confidence level are set following the CL_s prescription [53].

8.3 Exclusion limits on new diboson resonances

Limits on the production cross section times branching ratio of massive resonances are set in each diboson channel as a function of the resonance mass using the EGM W' as a benchmark for the WZ selection, and the bulk G_{RS} model for the WW and ZZ selections. In most of the mass range, the observed limit is somewhat better than the expected limit, but in the region near 2 TeV the excess of events in the data leads to observed limits which are weaker than expected. Figure 6a shows the observed 95% CL upper limits on the cross section times branching ratio on the EGM $W' \rightarrow WZ$ hypotheses as a function of

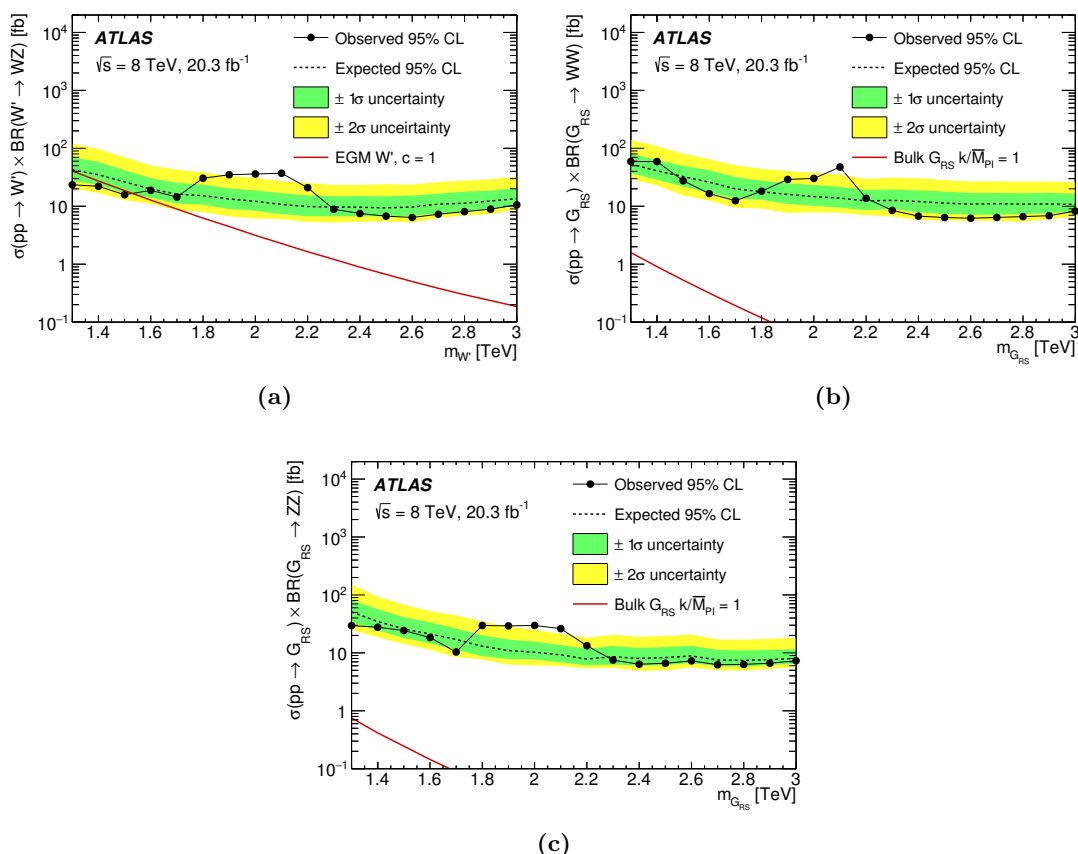


Figure 6. Upper limits, at 95% C.L., on the section times branching ratio limits for the WZ window selection as a function of $m_{W'}$, and for the WW window selection and the ZZ window selections as a function of $m_{G_{RS}}$. The solid red line in each figure displays the predicted cross section for the W' or G_{RS} model as a function of the resonance mass.

the W' mass. EGM $W' \rightarrow WZ$ for masses between 1.3 and 1.5 TeV are excluded at 95% CL. Figures 6b and 6c show the observed 95% CL upper limits on the cross section times branching ratio for the bulk $G_{RS} \rightarrow WW$ and ZZ , respectively. The cross section times branching ratio for excited graviton production with the model parameters described in section 3 is too low to be excluded with the sensitivity of this measurement.

9 Conclusions

A search has been performed for massive particles decaying to WW , WZ , or ZZ using 20.3 fb^{-1} of $\sqrt{s} = 8$ TeV pp collision data collected at the LHC by ATLAS in 2012. This is the first ATLAS search for resonant diboson production in a fully hadronic final state and strongly relies on the suppression of the dijet background with a substructure-based jet grooming and boson tagging procedure. The boson tagging selection includes different jet mass criteria to identify W and Z boson candidates and thus produces three overlapping sets of selected events for the searches in the WW , WZ , and ZZ decay channels. The

most significant discrepancy with the background-only model occurs around 2 TeV in the WZ channel with a local significance of 3.4σ and a global significance, taking the entire mass range of the search in all three channels into account, of 2.5σ .

Upper limits on the production cross section times branching ratio of massive resonances are set in each diboson channel as a function of the resonance mass, using an EGM $W' \rightarrow WZ$ as a benchmark for the WZ channel, and an excited bulk graviton G_{RS} to represent resonances decaying to WW and ZZ . A W' with EGM couplings and mass between 1.3 and 1.5 TeV is excluded at 95% CL.

Acknowledgments

We thank CERN for the very successful operation of the LHC, as well as the support staff from our institutions without whom ATLAS could not be operated efficiently.

We acknowledge the support of ANPCyT, Argentina; YerPhI, Armenia; ARC, Australia; BMWFW and FWF, Austria; ANAS, Azerbaijan; SSTC, Belarus; CNPq and FAPESP, Brazil; NSERC, NRC and CFI, Canada; CERN; CONICYT, Chile; CAS, MOST and NSFC, China; COLCIENCIAS, Colombia; MSMT CR, MPO CR and VSC CR, Czech Republic; DNRF, DNSRC and Lundbeck Foundation, Denmark; IN2P3-CNRS, CEA-DSM/IRFU, France; GNSF, Georgia; BMBF, HGF, and MPG, Germany; GSRT, Greece; RGC, Hong Kong SAR, China; ISF, I-CORE and Benoziyo Center, Israel; INFN, Italy; MEXT and JSPS, Japan; CNRST, Morocco; FOM and NWO, Netherlands; RCN, Norway; MNiSW and NCN, Poland; FCT, Portugal; MNE/IFA, Romania; MES of Russia and NRC KI, Russian Federation; JINR; MESTD, Serbia; MSSR, Slovakia; ARRS and MIZŠ, Slovenia; DST/NRF, South Africa; MINECO, Spain; SRC and Wallenberg Foundation, Sweden; SERI, SNSF and Cantons of Bern and Geneva, Switzerland; MOST, Taiwan; TAEK, Turkey; STFC, United Kingdom; DOE and NSF, United States of America. In addition, individual groups and members have received support from BCKDF, the Canada Council, CANARIE, CRC, Compute Canada, FQRNT, and the Ontario Innovation Trust, Canada; EPLANET, ERC, FP7, Horizon 2020 and Marie Skłodowska-Curie Actions, European Union; Investissements d’Avenir Labex and Idex, ANR, Region Auvergne and Fondation Partager le Savoir, France; DFG and AvH Foundation, Germany; Herakleitos, Thales and Aristeia programmes co-financed by EU-ESF and the Greek NSRF; BSF, GIF and Minerva, Israel; BRF, Norway; the Royal Society and Leverhulme Trust, United Kingdom.

The crucial computing support from all WLCG partners is acknowledged gratefully, in particular from CERN and the ATLAS Tier-1 facilities at TRIUMF (Canada), NDGF (Denmark, Norway, Sweden), CC-IN2P3 (France), KIT/GridKA (Germany), INFN-CNAF (Italy), NL-T1 (Netherlands), PIC (Spain), ASGC (Taiwan), RAL (U.K.) and BNL (U.S.A.) and in the Tier-2 facilities worldwide.

Open Access. This article is distributed under the terms of the Creative Commons Attribution License ([CC-BY 4.0](https://creativecommons.org/licenses/by/4.0/)), which permits any use, distribution and reproduction in any medium, provided the original author(s) and source are credited.

References

- [1] J.M. Butterworth, A.R. Davison, M. Rubin and G.P. Salam, *Jet substructure as a new Higgs search channel at the LHC*, *Phys. Rev. Lett.* **100** (2008) 242001 [[arXiv:0802.2470](#)] [[INSPIRE](#)].
- [2] E. Eichten and K. Lane, *Low-scale technicolor at the Tevatron and LHC*, *Phys. Lett. B* **669** (2008) 235 [[arXiv:0706.2339](#)] [[INSPIRE](#)].
- [3] S. Catterall, L. Del Debbio, J. Giedt and L. Keegan, *MCRG Minimal Walking Technicolor*, *Phys. Rev. D* **85** (2012) 094501 [[arXiv:1108.3794](#)] [[INSPIRE](#)].
- [4] J.R. Andersen et al., *Discovering Technicolor*, *Eur. Phys. J. Plus* **126** (2011) 81 [[arXiv:1104.1255](#)] [[INSPIRE](#)].
- [5] L. Randall and R. Sundrum, *A Large mass hierarchy from a small extra dimension*, *Phys. Rev. Lett.* **83** (1999) 3370 [[hep-ph/9905221](#)] [[INSPIRE](#)].
- [6] L. Randall and R. Sundrum, *An Alternative to compactification*, *Phys. Rev. Lett.* **83** (1999) 4690 [[hep-th/9906064](#)] [[INSPIRE](#)].
- [7] H. Davoudiasl, J.L. Hewett and T.G. Rizzo, *Experimental probes of localized gravity: On and off the wall*, *Phys. Rev. D* **63** (2001) 075004 [[hep-ph/0006041](#)] [[INSPIRE](#)].
- [8] J.C. Pati and A. Salam, *Lepton Number as the Fourth “Color”*, *Phys. Rev. D* **10** (1974) 275 [*Erratum ibid.* **D 11** (1975) 703] [[INSPIRE](#)].
- [9] H. Georgi and S.L. Glashow, *Unity of All Elementary Particle Forces*, *Phys. Rev. Lett.* **32** (1974) 438 [[INSPIRE](#)].
- [10] H. Georgi, *The State of the Art — Gauge Theories*, talk given at the 1974 Meeting of the Division of Particles and Fields of the APS, Williamsburg, Virginia, U.S.A., September 5–7 1974 [*AIP Conf. Proc.* **23** (1975) 575] [[INSPIRE](#)].
- [11] H. Fritzsch and P. Minkowski, *Unified Interactions of Leptons and Hadrons*, *Annals Phys.* **93** (1975) 193 [[INSPIRE](#)].
- [12] G. Altarelli, B. Mele and M. Ruiz-Altaba, *Searching for New Heavy Vector Bosons in $p\bar{p}$ Colliders*, *Z. Phys. C* **45** (1989) 109 [*Erratum ibid.* **C 47** (1990) 676] [[INSPIRE](#)].
- [13] E. Eichten, I. Hinchliffe, K.D. Lane and C. Quigg, *Super Collider Physics*, *Rev. Mod. Phys.* **56** (1984) 579 [[INSPIRE](#)].
- [14] C. Quigg, *Gauge Theories of the Strong, Weak, and Electromagnetic Interactions*, Princeton University Press (2013).
- [15] T. Han, J.D. Lykken and R.-J. Zhang, *On Kaluza-Klein states from large extra dimensions*, *Phys. Rev. D* **59** (1999) 105006 [[hep-ph/9811350](#)] [[INSPIRE](#)].
- [16] K. Agashe, H. Davoudiasl, G. Perez and A. Soni, *Warped Gravitons at the LHC and Beyond*, *Phys. Rev. D* **76** (2007) 036006 [[hep-ph/0701186](#)] [[INSPIRE](#)].
- [17] O. Antipin, D. Atwood and A. Soni, *Search for RS gravitons via $W_L W_L$ decays*, *Phys. Lett. B* **666** (2008) 155 [[arXiv:0711.3175](#)] [[INSPIRE](#)].
- [18] O. Antipin and A. Soni, *Towards establishing the spin of warped gravitons*, *JHEP* **10** (2008) 018 [[arXiv:0806.3427](#)] [[INSPIRE](#)].

- [19] CMS collaboration, *Search for massive resonances in dijet systems containing jets tagged as W or Z boson decays in pp collisions at $\sqrt{s} = 8$ TeV*, *JHEP* **08** (2014) 173 [[arXiv:1405.1994](#)] [[INSPIRE](#)].
- [20] CMS collaboration, *Search for massive resonances decaying into pairs of boosted bosons in semi-leptonic final states at $\sqrt{s} = 8$ TeV*, *JHEP* **08** (2014) 174 [[arXiv:1405.3447](#)] [[INSPIRE](#)].
- [21] ATLAS collaboration, *Search for resonant diboson production in the $\ell\ell q\bar{q}$ final state in pp collisions at $\sqrt{s} = 8$ TeV with the ATLAS detector*, *Eur. Phys. J. C* **75** (2015) 69 [[arXiv:1409.6190](#)] [[INSPIRE](#)].
- [22] ATLAS collaboration, *Search for production of WW/WZ resonances decaying to a lepton, neutrino and jets in pp collisions at $\sqrt{s} = 8$ TeV with the ATLAS detector*, *Eur. Phys. J. C* **75** (2015) 209 [Erratum *ibid.* **C 75** (2015) 370] [[arXiv:1503.04677](#)] [[INSPIRE](#)].
- [23] ATLAS collaboration, *The ATLAS Experiment at the CERN Large Hadron Collider*, 2008 *JINST* **3** S08003 [[INSPIRE](#)].
- [24] M. Cacciari, G.P. Salam and G. Soyez, *The Anti- k_t jet clustering algorithm*, *JHEP* **04** (2008) 063 [[arXiv:0802.1189](#)] [[INSPIRE](#)].
- [25] ATLAS collaboration, *Improved luminosity determination in pp collisions at $\sqrt{s} = 7$ TeV using the ATLAS detector at the LHC*, *Eur. Phys. J. C* **73** (2013) 2518 [[arXiv:1302.4393](#)] [[INSPIRE](#)].
- [26] T. Sjöstrand, S. Mrenna and P.Z. Skands, *A Brief Introduction to PYTHIA 8.1*, *Comput. Phys. Commun.* **178** (2008) 852 [[arXiv:0710.3820](#)] [[INSPIRE](#)].
- [27] T. Sjöstrand and P.Z. Skands, *Transverse-momentum-ordered showers and interleaved multiple interactions*, *Eur. Phys. J. C* **39** (2005) 129 [[hep-ph/0408302](#)] [[INSPIRE](#)].
- [28] T. Sjöstrand, S. Mrenna and P.Z. Skands, *PYTHIA 6.4 Physics and Manual*, *JHEP* **05** (2006) 026 [[hep-ph/0603175](#)] [[INSPIRE](#)].
- [29] A.D. Martin, W.J. Stirling, R.S. Thorne and G. Watt, *Parton distributions for the LHC*, *Eur. Phys. J. C* **63** (2009) 189 [[arXiv:0901.0002](#)] [[INSPIRE](#)].
- [30] ATLAS collaboration, *Further ATLAS tunes of PYTHIA6 and PYTHIA 8*, *ATL-PHYS-PUB-2011-014* (2011) [ATL-COM-PHYS-2011-1507] [[INSPIRE](#)].
- [31] B. Andersson, G. Gustafson, G. Ingelman and T. Sjöstrand, *Parton Fragmentation and String Dynamics*, *Phys. Rept.* **97** (1983) 31 [[INSPIRE](#)].
- [32] M. Bahr et al., *HERWIG++ Physics and Manual*, *Eur. Phys. J. C* **58** (2008) 639 [[arXiv:0803.0883](#)] [[INSPIRE](#)].
- [33] A. Belyaev, N.D. Christensen and A. Pukhov, *CalcHEP 3.4 for collider physics within and beyond the Standard Model*, *Comput. Phys. Commun.* **184** (2013) 1729 [[arXiv:1207.6082](#)] [[INSPIRE](#)].
- [34] D. Stump et al., *Inclusive jet production, parton distributions and the search for new physics*, *JHEP* **10** (2003) 046 [[hep-ph/0303013](#)] [[INSPIRE](#)].
- [35] S. Frixione and B.R. Webber, *Matching NLO QCD computations and parton shower simulations*, *JHEP* **06** (2002) 029 [[hep-ph/0204244](#)] [[INSPIRE](#)].
- [36] G. Corcella et al., *HERWIG 6: An Event generator for hadron emission reactions with interfering gluons (including supersymmetric processes)*, *JHEP* **01** (2001) 010 [[hep-ph/0011363](#)] [[INSPIRE](#)].

- [37] H.-L. Lai et al., *New parton distributions for collider physics*, *Phys. Rev. D* **82** (2010) 074024 [[arXiv:1007.2241](#)] [[INSPIRE](#)].
- [38] P. Nason, *A New method for combining NLO QCD with shower Monte Carlo algorithms*, *JHEP* **11** (2004) 040 [[hep-ph/0409146](#)] [[INSPIRE](#)].
- [39] ATLAS collaboration, *The ATLAS Simulation Infrastructure*, *Eur. Phys. J. C* **70** (2010) 823 [[arXiv:1005.4568](#)] [[INSPIRE](#)].
- [40] GEANT4 collaboration, S. Agostinelli et al., *GEANT4: A Simulation toolkit*, *Nucl. Instrum. Meth. A* **506** (2003) 250 [[INSPIRE](#)].
- [41] W. Lampl et al., *Calorimeter Clustering Algorithms: Description and Performance*, *ATL-LARG-PUB-2008-002* (2008) [ATL-COM-LARG-2008-003] [[INSPIRE](#)].
- [42] ATLAS LIQUID ARGON EMEC/HEC collaboration, C. Cojocaru et al., *Hadronic calibration of the ATLAS liquid argon end-cap calorimeter in the pseudorapidity region $1.6 < |\eta| < 1.8$ in beam tests*, *Nucl. Instrum. Meth. A* **531** (2004) 481 [[physics/0407009](#)] [[INSPIRE](#)].
- [43] Y.L. Dokshitzer, G.D. Leder, S. Moretti and B.R. Webber, *Better jet clustering algorithms*, *JHEP* **08** (1997) 001 [[hep-ph/9707323](#)] [[INSPIRE](#)].
- [44] M. Wobisch and T. Wengler, *Hadronization corrections to jet cross-sections in deep inelastic scattering*, PITHA-99-16 [[hep-ph/9907280](#)] [[INSPIRE](#)].
- [45] M. Cacciari, G.P. Salam and G. Soyez, *FastJet User Manual*, *Eur. Phys. J. C* **72** (2012) 1896 [[arXiv:1111.6097](#)] [[INSPIRE](#)].
- [46] M. Cacciari, G.P. Salam and G. Soyez, *The Catchment Area of Jets*, *JHEP* **04** (2008) 005 [[arXiv:0802.1188](#)] [[INSPIRE](#)].
- [47] ATLAS collaboration, *Performance of jet substructure techniques for large- R jets in proton-proton collisions at $\sqrt{s} = 7$ TeV using the ATLAS detector*, *JHEP* **09** (2013) 076 [[arXiv:1306.4945](#)] [[INSPIRE](#)].
- [48] ATLAS collaboration, *Search for dark matter in events with a hadronically decaying W or Z boson and missing transverse momentum in pp collisions at $\sqrt{s} = 8$ TeV with the ATLAS detector*, *Phys. Rev. Lett.* **112** (2014) 041802 [[arXiv:1309.4017](#)] [[INSPIRE](#)].
- [49] G. Choudalakis and D. Casadei, *Plotting the differences between data and expectation*, *Eur. Phys. J. Plus* **127** (2012) 25 [[arXiv:1111.2062](#)].
- [50] ATLAS collaboration, *Light-quark and gluon jet discrimination in pp collisions at $\sqrt{s} = 7$ TeV with the ATLAS detector*, *Eur. Phys. J. C* **74** (2014) 3023 [[arXiv:1405.6583](#)] [[INSPIRE](#)].
- [51] M. Botje et al., *The PDF4LHC Working Group Interim Recommendations*, [arXiv:1101.0538](#) [[INSPIRE](#)].
- [52] G. Cowan, K. Cranmer, E. Gross and O. Vitells, *Asymptotic formulae for likelihood-based tests of new physics*, *Eur. Phys. J. C* **71** (2011) 1554 [Erratum *ibid.* **C 73** (2013) 2501] [[arXiv:1007.1727](#)] [[INSPIRE](#)].
- [53] A.L. Read, *Presentation of search results: The CL_s technique*, *J. Phys. G* **28** (2002) 2693 [[INSPIRE](#)].

The ATLAS collaboration

G. Aad⁸⁵, B. Abbott¹¹³, J. Abdallah¹⁵¹, O. Abdinov¹¹, R. Aben¹⁰⁷, M. Abolins⁹⁰, O.S. AbouZeid¹⁵⁸, H. Abramowicz¹⁵³, H. Abreu¹⁵², R. Abreu³⁰, Y. Abulaiti^{146a,146b}, B.S. Acharya^{164a,164b,a}, L. Adamczyk^{38a}, D.L. Adams²⁵, J. Adelman¹⁰⁸, S. Adomeit¹⁰⁰, T. Adye¹³¹, A.A. Affolder⁷⁴, T. Agatonovic-Jovin¹³, J.A. Aguilar-Saavedra^{126a,126f}, S.P. Ahlen²², F. Ahmadov^{65,b}, G. Aielli^{133a,133b}, H. Akerstedt^{146a,146b}, T.P.A. Åkesson⁸¹, G. Akimoto¹⁵⁵, A.V. Akimov⁹⁶, G.L. Alberghi^{20a,20b}, J. Albert¹⁶⁹, S. Albrand⁵⁵, M.J. Alconada Verzini⁷¹, M. Aleksa³⁰, I.N. Aleksandrov⁶⁵, C. Alexa^{26a}, G. Alexander¹⁵³, T. Alexopoulos¹⁰, M. Alhroob¹¹³, G. Alimonti^{91a}, L. Alio⁸⁵, J. Alison³¹, S.P. Alkire³⁵, B.M.M. Allbrooke¹⁸, P.P. Allport⁷⁴, A. Aloisio^{104a,104b}, A. Alonso³⁶, F. Alonso⁷¹, C. Alpigiani⁷⁶, A. Altheimer³⁵, B. Alvarez Gonzalez³⁰, D. Álvarez Piqueras¹⁶⁷, M.G. Alvigi^{104a,104b}, B.T. Amadio¹⁵, K. Amako⁶⁶, Y. Amaral Coutinho^{24a}, C. Amelung²³, D. Amidei⁸⁹, S.P. Amor Dos Santos^{126a,126c}, A. Amorim^{126a,126b}, S. Amoroso⁴⁸, N. Amram¹⁵³, G. Amundsen²³, C. Anastopoulos¹³⁹, L.S. Ancu⁴⁹, N. Andari³⁰, T. Andeen³⁵, C.F. Anders^{58b}, G. Anders³⁰, J.K. Anders⁷⁴, K.J. Anderson³¹, A. Andreazza^{91a,91b}, V. Andrei^{58a}, S. Angelidakis⁹, I. Angelozzi¹⁰⁷, P. Anger⁴⁴, A. Angerami³⁵, F. Anghinolfi³⁰, A.V. Anisenkov^{109,c}, N. Anjos¹², A. Annovi^{124a,124b}, M. Antonelli⁴⁷, A. Antonov⁹⁸, J. Antos^{144b}, F. Anulli^{132a}, M. Aoki⁶⁶, L. Aperio Bella¹⁸, G. Arabidze⁹⁰, Y. Arai⁶⁶, J.P. Araque^{126a}, A.T.H. Arce⁴⁵, F.A. Arduh⁷¹, J-F. Arguin⁹⁵, S. Argyropoulos⁴², M. Arik^{19a}, A.J. Armbruster³⁰, O. Arnaez³⁰, V. Arnal⁸², H. Arnold⁴⁸, M. Arratia²⁸, O. Arslan²¹, A. Artamonov⁹⁷, G. Artoni²³, S. Asai¹⁵⁵, N. Asbah⁴², A. Ashkenazi¹⁵³, B. Åsman^{146a,146b}, L. Asquith¹⁴⁹, K. Assamagan²⁵, R. Astalos^{144a}, M. Atkinson¹⁶⁵, N.B. Atlay¹⁴¹, B. Auerbach⁶, K. Augsten¹²⁸, M. Aourousseau^{145b}, G. Avolio³⁰, B. Axen¹⁵, M.K. Ayoub¹¹⁷, G. Azuelos^{95,d}, M.A. Baak³⁰, A.E. Baas^{58a}, C. Bacci^{134a,134b}, H. Bachacou¹³⁶, K. Bachas¹⁵⁴, M. Backes³⁰, M. Backhaus³⁰, P. Bagiachi^{132a,132b}, P. Bagnaia^{132a,132b}, Y. Bai^{33a}, T. Bain³⁵, J.T. Baines¹³¹, O.K. Baker¹⁷⁶, P. Balek¹²⁹, T. Balestri¹⁴⁸, F. Balli⁸⁴, E. Banas³⁹, Sw. Banerjee¹⁷³, A.A.E. Bannoura¹⁷⁵, H.S. Bansil¹⁸, L. Barak³⁰, E.L. Barberio⁸⁸, D. Barberis^{50a,50b}, M. Barbero⁸⁵, T. Barillari¹⁰¹, M. Barisonzi^{164a,164b}, T. Barklow¹⁴³, N. Barlow²⁸, S.L. Barnes⁸⁴, B.M. Barnett¹³¹, R.M. Barnett¹⁵, Z. Barnovska⁵, A. Baroncelli^{134a}, G. Barone⁴⁹, A.J. Barr¹²⁰, F. Barreiro⁸², J. Barreiro Guimarães da Costa⁵⁷, R. Bartoldus¹⁴³, A.E. Barton⁷², P. Bartos^{144a}, A. Basalaeu¹²³, A. Bassalat¹¹⁷, A. Basye¹⁶⁵, R.L. Bates⁵³, S.J. Batista¹⁵⁸, J.R. Batley²⁸, M. Battaglia¹³⁷, M. Bauce^{132a,132b}, F. Bauer¹³⁶, H.S. Bawa^{143,e}, J.B. Beacham¹¹¹, M.D. Beattie⁷², T. Beau⁸⁰, P.H. Beauchemin¹⁶¹, R. Beccherle^{124a,124b}, P. Bechtel²¹, H.P. Beck^{17,f}, K. Becker¹²⁰, M. Becker⁸³, S. Becker¹⁰⁰, M. Beckingham¹⁷⁰, C. Becot¹¹⁷, A.J. Beddall^{19c}, A. Beddall^{19c}, V.A. Bednyakov⁶⁵, C.P. Bee¹⁴⁸, L.J. Beemster¹⁰⁷, T.A. Beermann¹⁷⁵, M. Begel²⁵, J.K. Behr¹²⁰, C. Belanger-Champagne⁸⁷, W.H. Bell⁴⁹, G. Bella¹⁵³, L. Bellagamba^{20a}, A. Bellerive²⁹, M. Bellomo⁸⁶, K. Belotskiy⁹⁸, O. Beltramello³⁰, O. Benary¹⁵³, D. Bencheikroun^{135a}, M. Bender¹⁰⁰, K. Bendtz^{146a,146b}, N. Benekos¹⁰, Y. Benhammou¹⁵³, E. Benhar Noccioli⁴⁹, J.A. Benitez Garcia^{159b}, D.P. Benjamin⁴⁵, J.R. Bensinger²³, S. Bentvelsen¹⁰⁷, L. Beresford¹²⁰, M. Beretta⁴⁷, D. Berge¹⁰⁷, E. Bergeas Kuutmann¹⁶⁶, N. Berger⁵, F. Berghaus¹⁶⁹, J. Beringer¹⁵, C. Bernard²², N.R. Bernard⁸⁶, C. Bernius¹¹⁰, F.U. Bernlochner²¹, T. Berry⁷⁷, P. Berta¹²⁹, C. Bertella⁸³, G. Bertoli^{146a,146b}, F. Bertolucci^{124a,124b}, C. Bertsche¹¹³, D. Bertsche¹¹³, M.I. Besana^{91a}, G.J. Besjes¹⁰⁶, O. Bessidskaia Bylund^{146a,146b}, M. Bessner⁴², N. Besson¹³⁶, C. Betancourt⁴⁸, S. Bethke¹⁰¹, A.J. Bevan⁷⁶, W. Bhimji⁴⁶, R.M. Bianchi¹²⁵, L. Bianchini²³, M. Bianco³⁰, O. Biebel¹⁰⁰, D. Biedermann¹⁶, S.P. Bieniek⁷⁸, M. Biglietti^{134a}, J. Bilbao De Mendizabal⁴⁹, H. Bilokon⁴⁷, M. Bindi⁵⁴, S. Binet¹¹⁷, A. Bingul^{19c}, C. Bini^{132a,132b}, C.W. Black¹⁵⁰, J.E. Black¹⁴³, K.M. Black²², D. Blackburn¹³⁸, R.E. Blair⁶, J.-B. Blanchard¹³⁶, J.E. Blanco⁷⁷, T. Blazek^{144a}, I. Bloch⁴², C. Blocker²³, W. Blum^{83,*}, U. Blumenschein⁵⁴, G.J. Bobbink¹⁰⁷, V.S. Bobrovnikov^{109,c}, S.S. Bocchetta⁸¹, A. Bocci⁴⁵, C. Bock¹⁰⁰, M. Boehler⁴⁸,

J.A. Bogaerts³⁰, D. Bogavac¹³, A.G. Bogdanchikov¹⁰⁹, C. Bohm^{146a}, V. Boisvert⁷⁷, T. Bold^{38a},
 V. Boldea^{26a}, A.S. Boldyrev⁹⁹, M. Bomben⁸⁰, M. Bona⁷⁶, M. Boonekamp¹³⁶, A. Borisov¹³⁰,
 G. Borissov⁷², S. Borroni⁴², J. Bortfeldt¹⁰⁰, V. Bortolotto^{60a,60b,60c}, K. Bos¹⁰⁷, D. Boscherini^{20a},
 M. Bosman¹², J. Boudreau¹²⁵, J. Bouffard², E.V. Bouhova-Thacker⁷², D. Boumediene³⁴,
 C. Bourdarios¹¹⁷, N. Bousson¹¹⁴, A. Boveia³⁰, J. Boyd³⁰, I.R. Boyko⁶⁵, I. Bozic¹³, J. Bracinik¹⁸,
 A. Brandt⁸, G. Brandt⁵⁴, O. Brandt^{58a}, U. Bratzler¹⁵⁶, B. Brau⁸⁶, J.E. Brau¹¹⁶, H.M. Braun^{175,*},
 S.F. Brazzale^{164a,164c}, W.D. Breaden Madden⁵³, K. Brendlinger¹²², A.J. Brennan⁸⁸,
 L. Brenner¹⁰⁷, R. Brenner¹⁶⁶, S. Bressler¹⁷², K. Bristow^{145c}, T.M. Bristow⁴⁶, D. Britton⁵³,
 D. Britzger⁴², F.M. Brochu²⁸, I. Brock²¹, R. Brock⁹⁰, J. Bronner¹⁰¹, G. Brooijmans³⁵,
 T. Brooks⁷⁷, W.K. Brooks^{32b}, J. Brosamer¹⁵, E. Brost¹¹⁶, J. Brown⁵⁵,
 P.A. Bruckman de Renstrom³⁹, D. Bruncko^{144b}, R. Bruneliere⁴⁸, A. Bruni^{20a}, G. Bruni^{20a},
 M. Bruschi^{20a}, N. Brusino²¹, L. Bryngemark⁸¹, T. Buanes¹⁴, Q. Buat¹⁴², P. Buchholz¹⁴¹,
 A.G. Buckley⁵³, S.I. Buda^{26a}, I.A. Budagov⁶⁵, F. Buehrer⁴⁸, L. Bugge¹¹⁹, M.K. Bugge¹¹⁹,
 O. Bulekov⁹⁸, D. Bullock⁸, H. Burckhart³⁰, S. Burdin⁷⁴, B. Burgrave¹⁰⁸, S. Burke¹³¹,
 I. Burmeister⁴³, E. Busato³⁴, D. Büscher⁴⁸, V. Büscher⁸³, P. Bussey⁵³, J.M. Butler²², A.I. Butt³,
 C.M. Buttar⁵³, J.M. Butterworth⁷⁸, P. Butti¹⁰⁷, W. Buttinger²⁵, A. Buzatu⁵³,
 A.R. Buzykaev^{109,c}, S. Cabrera Urbán¹⁶⁷, D. Caforio¹²⁸, V.M. Cairo^{37a,37b}, O. Cakir^{4a},
 P. Calafiura¹⁵, A. Calandri¹³⁶, G. Calderini⁸⁰, P. Calfayan¹⁰⁰, L.P. Caloba^{24a}, D. Calvet³⁴,
 S. Calvet³⁴, R. Camacho Toro³¹, S. Camarda⁴², P. Camarri^{133a,133b}, D. Cameron¹¹⁹,
 L.M. Caminada¹⁵, R. Caminal Armadans¹⁶⁵, S. Campana³⁰, M. Campanelli⁷⁸, A. Campoverde¹⁴⁸,
 V. Canale^{104a,104b}, A. Canepa^{159a}, M. Cano Bret⁷⁶, J. Cantero⁸², R. Cantrill^{126a}, T. Cao⁴⁰,
 M.D.M. Capeans Garrido³⁰, I. Caprini^{26a}, M. Caprini^{26a}, M. Capua^{37a,37b}, R. Caputo⁸³,
 R. Cardarelli^{133a}, F. Cardillo⁴⁸, T. Carli³⁰, G. Carlino^{104a}, L. Carminati^{91a,91b}, S. Caron¹⁰⁶,
 E. Carquin^{32a}, G.D. Carrillo-Montoya⁸, J.R. Carter²⁸, J. Carvalho^{126a,126c}, D. Casadei⁷⁸,
 M.P. Casado¹², M. Casolino¹², E. Castaneda-Miranda^{145b}, A. Castelli¹⁰⁷, V. Castillo Gimenez¹⁶⁷,
 N.F. Castro^{126a,g}, P. Catastini⁵⁷, A. Catinaccio³⁰, J.R. Catmore¹¹⁹, A. Cattai³⁰, J. Caudron⁸³,
 V. Cavaliere¹⁶⁵, D. Cavalli^{91a}, M. Cavalli-Sforza¹², V. Cavasinni^{124a,124b}, F. Ceradini^{134a,134b},
 B.C. Cerio⁴⁵, K. Cerny¹²⁹, A.S. Cerqueira^{24b}, A. Cerri¹⁴⁹, L. Cerrito⁷⁶, F. Cerutti¹⁵, M. Cerv³⁰,
 A. Cervelli¹⁷, S.A. Cetin^{19b}, A. Chafaq^{135a}, D. Chakraborty¹⁰⁸, I. Chalupkova¹²⁹, P. Chang¹⁶⁵,
 B. Chapleau⁸⁷, J.D. Chapman²⁸, D.G. Charlton¹⁸, C.C. Chau¹⁵⁸, C.A. Chavez Barajas¹⁴⁹,
 S. Cheatham¹⁵², A. Chegwidan⁹⁰, S. Chekanov⁶, S.V. Chekulaev^{159a}, G.A. Chelkov^{65,h},
 M.A. Chelstowska⁸⁹, C. Chen⁶⁴, H. Chen²⁵, K. Chen¹⁴⁸, L. Chen^{33d,i}, S. Chen^{33c}, X. Chen^{33f},
 Y. Chen⁶⁷, H.C. Cheng⁸⁹, Y. Cheng³¹, A. Cheplakov⁶⁵, E. Cheremushkina¹³⁰,
 R. Cherkouki El Moursli^{135e}, V. Chernyatin^{25,*}, E. Cheu⁷, L. Chevalier¹³⁶, V. Chiarella⁴⁷,
 J.T. Childers⁶, G. Chiodini^{73a}, A.S. Chisholm¹⁸, R.T. Chislett⁷⁸, A. Chitan^{26a}, M.V. Chizhov⁶⁵,
 K. Choi⁶¹, S. Chouridou⁹, B.K.B. Chow¹⁰⁰, V. Christodoulou⁷⁸, D. Chromek-Burckhart³⁰,
 J. Chudoba¹²⁷, A.J. Chuinard⁸⁷, J.J. Chwastowski³⁹, L. Chytka¹¹⁵, G. Ciapetti^{132a,132b},
 A.K. Ciftci^{4a}, D. Cinca⁵³, V. Cindro⁷⁵, I.A. Cioara²¹, A. Ciocio¹⁵, Z.H. Citron¹⁷²,
 M. Ciubancan^{26a}, A. Clark⁴⁹, B.L. Clark⁵⁷, P.J. Clark⁴⁶, R.N. Clarke¹⁵, W. Cleland¹²⁵,
 C. Clement^{146a,146b}, Y. Coadou⁸⁵, M. Cobal^{164a,164c}, A. Coccaro¹³⁸, J. Cochran⁶⁴, L. Coffey²³,
 J.G. Cogan¹⁴³, B. Cole³⁵, S. Cole¹⁰⁸, A.P. Colijn¹⁰⁷, J. Collot⁵⁵, T. Colombo^{58c},
 G. Compostella¹⁰¹, P. Conde Muiño^{126a,126b}, E. Coniavitis⁴⁸, S.H. Connell^{145b}, I.A. Connolly⁷⁷,
 S.M. Consonni^{91a,91b}, V. Consorti⁴⁸, S. Constantinescu^{26a}, C. Conta^{121a,121b}, G. Conti³⁰,
 F. Conventi^{104a,j}, M. Cooke¹⁵, B.D. Cooper⁷⁸, A.M. Cooper-Sarkar¹²⁰, T. Cornelissen¹⁷⁵,
 M. Corradi^{20a}, F. Corriveau^{87,k}, A. Corso-Radu¹⁶³, A. Cortes-Gonzalez¹², G. Cortiana¹⁰¹,
 G. Costa^{91a}, M.J. Costa¹⁶⁷, D. Costanzo¹³⁹, D. Côté⁸, G. Cottin²⁸, G. Cowan⁷⁷, B.E. Cox⁸⁴,
 K. Cranmer¹¹⁰, G. Cree²⁹, S. Crépe-Renaudin⁵⁵, F. Crescioli⁸⁰, W.A. Cribbs^{146a,146b},
 M. Crispin Ortuzar¹²⁰, M. Cristinziani²¹, V. Croft¹⁰⁶, G. Crosetti^{37a,37b},
 T. Cuhadar Donszelmann¹³⁹, J. Cummings¹⁷⁶, M. Curatolo⁴⁷, C. Cuthbert¹⁵⁰, H. Czirr¹⁴¹,

P. Czodrowski³, S. D'Auria⁵³, M. D'Onofrio⁷⁴, M.J. Da Cunha Sargedas De Sousa^{126a,126b},
 C. Da Via⁸⁴, W. Dabrowski^{38a}, A. Dafinca¹²⁰, T. Dai⁸⁹, O. Dale¹⁴, F. Dallaire⁹⁵,
 C. Dallapiccola⁸⁶, M. Dam³⁶, J.R. Dandoy³¹, N.P. Dang⁴⁸, A.C. Daniells¹⁸, M. Danninger¹⁶⁸,
 M. Dano Hoffmann¹³⁶, V. Dao⁴⁸, G. Darbo^{50a}, S. Darmora⁸, J. Dassoulas³, A. Dattagupta⁶¹,
 W. Davey²¹, C. David¹⁶⁹, T. Davidek¹²⁹, E. Davies^{120,l}, M. Davies¹⁵³, P. Davison⁷⁸,
 Y. Davygora^{58a}, E. Dawe⁸⁸, I. Dawson¹³⁹, R.K. Daya-Ishmukhametova⁸⁶, K. De⁸,
 R. de Asmundis^{104a}, S. De Castro^{20a,20b}, S. De Cecco⁸⁰, N. De Groot¹⁰⁶, P. de Jong¹⁰⁷,
 H. De la Torre⁸², F. De Lorenzi⁶⁴, L. De Nooij¹⁰⁷, D. De Pedis^{132a}, A. De Salvo^{132a},
 U. De Sanctis¹⁴⁹, A. De Santo¹⁴⁹, J.B. De Vivie De Regie¹¹⁷, W.J. Dearnaley⁷², R. Debbé²⁵,
 C. Debenedetti¹³⁷, D.V. Dedovich⁶⁵, I. Deigaard¹⁰⁷, J. Del Peso⁸², T. Del Prete^{124a,124b},
 D. Delgove¹¹⁷, F. Deliot¹³⁶, C.M. Delitzsch⁴⁹, M. Deliyergiyev⁷⁵, A. Dell'Acqua³⁰, L. Dell'Asta²²,
 M. Dell'Orso^{124a,124b}, M. Della Pietra^{104a,j}, D. della Volpe⁴⁹, M. Delmastro⁵, P.A. Delsart⁵⁵,
 C. Deluca¹⁰⁷, D.A. DeMarco¹⁵⁸, S. Demers¹⁷⁶, M. Demichev⁶⁵, A. Demilly⁸⁰, S.P. Denisov¹³⁰,
 D. Derendarz³⁹, J.E. Derkaoui^{135d}, F. Derue⁸⁰, P. Dervan⁷⁴, K. Desch²¹, C. Deterre⁴²,
 P.O. Deviveiros³⁰, A. Dewhurst¹³¹, S. Dhaliwal²³, A. Di Ciaccio^{133a,133b}, L. Di Ciaccio⁵,
 A. Di Domenico^{132a,132b}, C. Di Donato^{104a,104b}, A. Di Girolamo³⁰, B. Di Girolamo³⁰,
 A. Di Mattia¹⁵², B. Di Micco^{134a,134b}, R. Di Nardo⁴⁷, A. Di Simone⁴⁸, R. Di Sipio¹⁵⁸,
 D. Di Valentino²⁹, C. Diaconu⁸⁵, M. Diamond¹⁵⁸, F.A. Dias⁴⁶, M.A. Diaz^{32a}, E.B. Diehl⁸⁹,
 J. Dietrich¹⁶, S. Diglio⁸⁵, A. Dimitrievska¹³, J. Dingfelder²¹, P. Dita^{26a}, S. Dita^{26a}, F. Dittus³⁰,
 F. Djama⁸⁵, T. Djobava^{51b}, J.I. Djuvsland^{58a}, M.A.B. do Vale^{24c}, D. Dobos³⁰, M. Dobre^{26a},
 C. Doglioni⁴⁹, T. Dohmae¹⁵⁵, J. Dolejsi¹²⁹, Z. Dolezal¹²⁹, B.A. Dolgoshein^{98,*}, M. Donadelli^{24d},
 S. Donati^{124a,124b}, P. Dondero^{121a,121b}, J. Donini³⁴, J. Dopke¹³¹, A. Doria^{104a}, M.T. Dova⁷¹,
 A.T. Doyle⁵³, E. Drechsler⁵⁴, M. Dris¹⁰, E. Dubreuil³⁴, E. Duchovni¹⁷², G. Duckeck¹⁰⁰,
 O.A. Ducu^{26a,85}, D. Duda¹⁷⁵, A. Dudarev³⁰, L. Duflot¹¹⁷, L. Duguid⁷⁷, M. Dührssen³⁰,
 M. Dunford^{58a}, H. Duran Yildiz^{4a}, M. Düren⁵², A. Durglishvili^{51b}, D. Duschinger⁴⁴,
 M. Dyndal^{38a}, C. Eckardt⁴², K.M. Ecker¹⁰¹, R.C. Edgar⁸⁹, W. Edson², N.C. Edwards⁴⁶,
 W. Ehrenfeld²¹, T. Eifert³⁰, G. Eigen¹⁴, K. Einsweiler¹⁵, T. Ekelof¹⁶⁶, M. El Kacimi^{135c},
 M. Ellert¹⁶⁶, S. Elles⁵, F. Ellinghaus⁸³, A.A. Elliot¹⁶⁹, N. Ellis³⁰, J. Elmsheuser¹⁰⁰, M. Elsing³⁰,
 D. Emelianov¹³¹, Y. Enari¹⁵⁵, O.C. Endner⁸³, M. Endo¹¹⁸, J. Erdmann⁴³, A. Ereditato¹⁷,
 G. Ernis¹⁷⁵, J. Ernst², M. Ernst²⁵, S. Errede¹⁶⁵, E. Ertel⁸³, M. Escalier¹¹⁷, H. Esch⁴³,
 C. Escobar¹²⁵, B. Esposito⁴⁷, A.I. Etievre¹³⁶, E. Etzion¹⁵³, H. Evans⁶¹, A. Ezhilov¹²³,
 L. Fabbri^{20a,20b}, G. Facini³¹, R.M. Fakhrudinov¹³⁰, S. Falciano^{132a}, R.J. Falla⁷⁸, J. Faltova¹²⁹,
 Y. Fang^{33a}, M. Fanti^{91a,91b}, A. Farbin⁸, A. Farilla^{134a}, T. Farooque¹², S. Farrell¹⁵,
 S.M. Farrington¹⁷⁰, P. Farthouat³⁰, F. Fassi^{135e}, P. Fassnacht³⁰, D. Fassouliotis⁹,
 M. Fauci Giannelli⁷⁷, A. Favareto^{50a,50b}, L. Fayard¹¹⁷, P. Federic^{144a}, O.L. Fedin^{123,m},
 W. Fedorko¹⁶⁸, S. Feigl³⁰, L. Feligioni⁸⁵, C. Feng^{33d}, E.J. Feng⁶, H. Feng⁸⁹, A.B. Fenyuk¹³⁰,
 L. Feremenga⁸, P. Fernandez Martinez¹⁶⁷, S. Fernandez Perez³⁰, J. Ferrando⁵³, A. Ferrari¹⁶⁶,
 P. Ferrari¹⁰⁷, R. Ferrari^{121a}, D.E. Ferreira de Lima⁵³, A. Ferrer¹⁶⁷, D. Ferrere⁴⁹, C. Ferretti⁸⁹,
 A. Ferretto Parodi^{50a,50b}, M. Fiascaris³¹, F. Fiedler⁸³, A. Filipčić⁷⁵, M. Filipuzzi⁴², F. Filthaut¹⁰⁶,
 M. Fincke-Keeler¹⁶⁹, K.D. Finelli¹⁵⁰, M.C.N. Fiolhais^{126a,126c}, L. Fiorini¹⁶⁷, A. Firan⁴⁰,
 A. Fischer², C. Fischer¹², J. Fischer¹⁷⁵, W.C. Fisher⁹⁰, E.A. Fitzgerald²³, I. Fleck¹⁴¹,
 P. Fleischmann⁸⁹, S. Fleischmann¹⁷⁵, G.T. Fletcher¹³⁹, G. Fletcher⁷⁶, R.R.M. Fletcher¹²²,
 T. Flick¹⁷⁵, A. Floderus⁸¹, L.R. Flores Castillo^{60a}, M.J. Flowerdew¹⁰¹, A. Formica¹³⁶, A. Forti⁸⁴,
 D. Fournier¹¹⁷, H. Fox⁷², S. Fracchia¹², P. Francavilla⁸⁰, M. Franchini^{20a,20b}, D. Francis³⁰,
 L. Franconi¹¹⁹, M. Franklin⁵⁷, M. Frate¹⁶³, M. Fraternali^{121a,121b}, D. Freeborn⁷⁸, S.T. French²⁸,
 F. Friedrich⁴⁴, D. Froidevaux³⁰, J.A. Frost¹²⁰, C. Fukunaga¹⁵⁶, E. Fullana Torregrosa⁸³,
 B.G. Fulsom¹⁴³, J. Fuster¹⁶⁷, C. Gabaldon⁵⁵, O. Gabizon¹⁷⁵, A. Gabrielli^{20a,20b},
 A. Gabrielli^{132a,132b}, S. Gadatsch¹⁰⁷, S. Gadomski⁴⁹, G. Gagliardi^{50a,50b}, P. Gagnon⁶¹,
 C. Galea¹⁰⁶, B. Galhardo^{126a,126c}, E.J. Gallas¹²⁰, B.J. Gallop¹³¹, P. Gallus¹²⁸, G. Galster³⁶,

K.K. Gan¹¹¹, J. Gao^{33b,85}, Y. Gao⁴⁶, Y.S. Gao^{143,e}, F.M. Garay Walls⁴⁶, F. Garberson¹⁷⁶,
 C. García¹⁶⁷, J.E. García Navarro¹⁶⁷, M. Garcia-Sciveres¹⁵, R.W. Gardner³¹, N. Garelli¹⁴³,
 V. Garonne¹¹⁹, C. Gatti⁴⁷, A. Gaudiello^{50a,50b}, G. Gaudio^{121a}, B. Gaur¹⁴¹, L. Gauthier⁹⁵,
 P. Gauzzi^{132a,132b}, I.L. Gavrilenko⁹⁶, C. Gay¹⁶⁸, G. Gaycken²¹, E.N. Gazis¹⁰, P. Ge^{33d},
 Z. Gecse¹⁶⁸, C.N.P. Gee¹³¹, D.A.A. Geerts¹⁰⁷, Ch. Geich-Gimbel²¹, M.P. Geisler^{58a}, C. Gemme^{50a},
 M.H. Genest⁵⁵, S. Gentile^{132a,132b}, M. George⁵⁴, S. George⁷⁷, D. Gerbaudo¹⁶³, A. Gershon¹⁵³,
 H. Ghazlane^{135b}, B. Giacobbe^{20a}, S. Giagu^{132a,132b}, V. Giangiobbe¹², P. Giannetti^{124a,124b},
 B. Gibbard²⁵, S.M. Gibson⁷⁷, M. Gilchriese¹⁵, T.P.S. Gillam²⁸, D. Gillberg³⁰, G. Gilles³⁴,
 D.M. Gingrich^{3,d}, N. Giokaris⁹, M.P. Giordani^{164a,164c}, F.M. Giorgi^{20a}, F.M. Giorgi¹⁶,
 P.F. Giraud¹³⁶, P. Giromini⁴⁷, D. Giugni^{91a}, C. Giuliani⁴⁸, M. Giulini^{58b}, B.K. Gjelsten¹¹⁹,
 S. Gkaitatzis¹⁵⁴, I. Gkialas¹⁵⁴, E.L. Gkougkousis¹¹⁷, L.K. Gladilin⁹⁹, C. Glasman⁸², J. Glatzer³⁰,
 P.C.F. Glaysheer⁴⁶, A. Glazov⁴², M. Goblirsch-Kolb¹⁰¹, J.R. Goddard⁷⁶, J. Godlewski³⁹,
 S. Goldfarb⁸⁹, T. Golling⁴⁹, D. Golubkov¹³⁰, A. Gomes^{126a,126b,126d}, R. Gonçalo^{126a},
 J. Goncalves Pinto Firmino Da Costa¹³⁶, L. Gonella²¹, S. González de la Hoz¹⁶⁷,
 G. Gonzalez Parra¹², S. Gonzalez-Sevilla⁴⁹, L. Goossens³⁰, P.A. Gorbounov⁹⁷, H.A. Gordon²⁵,
 I. Gorelov¹⁰⁵, B. Gorini³⁰, E. Gorini^{73a,73b}, A. Gorišek⁷⁵, E. Gornicki³⁹, A.T. Goshaw⁴⁵,
 C. Gössling⁴³, M.I. Gostkin⁶⁵, D. Goujdami^{135c}, A.G. Goussiou¹³⁸, N. Govender^{145b},
 E. Gozani¹⁵², H.M.X. Grabas¹³⁷, L. Graber⁵⁴, I. Grabowska-Bold^{38a}, P. Grafström^{20a,20b},
 K.-J. Grahm⁴², J. Gramling⁴⁹, E. Gramstad¹¹⁹, S. Grancagnolo¹⁶, V. Grassi¹⁴⁸, V. Gratchev¹²³,
 H.M. Gray³⁰, E. Graziani^{134a}, Z.D. Greenwood^{79,n}, K. Gregersen⁷⁸, I.M. Gregor⁴², P. Grenier¹⁴³,
 J. Griffiths⁸, A.A. Grillo¹³⁷, K. Grimm⁷², S. Grinstein^{12,o}, Ph. Gris³⁴, J.-F. Grivaz¹¹⁷,
 J.P. Grohs⁴⁴, A. Grohsjean⁴², E. Gross¹⁷², J. Grosse-Knetter⁵⁴, G.C. Grossi⁷⁹, Z.J. Grout¹⁴⁹,
 L. Guan^{33b}, J. Guenther¹²⁸, F. Guescini⁴⁹, D. Guest¹⁷⁶, O. Gueta¹⁵³, E. Guido^{50a,50b},
 T. Guillemin¹¹⁷, S. Guindon², U. Gul⁵³, C. Gumpert⁴⁴, J. Guo^{33e}, S. Gupta¹²⁰,
 G. Gustavino^{132a,132b}, P. Gutierrez¹¹³, N.G. Gutierrez Ortiz⁵³, C. Gutsche⁴⁴, C. Guyot¹³⁶,
 C. Gwenlan¹²⁰, C.B. Gwilliam⁷⁴, A. Haas¹¹⁰, C. Haber¹⁵, H.K. Hadavand⁸, N. Haddad^{135e},
 P. Haefner²¹, S. Hageböck²¹, Z. Hajduk³⁹, H. Hakobyan¹⁷⁷, M. Haleem⁴², J. Haley¹¹⁴, D. Hall¹²⁰,
 G. Halladjian⁹⁰, G.D. Hallewell⁸⁵, K. Hamacher¹⁷⁵, P. Hamal¹¹⁵, K. Hamano¹⁶⁹, M. Hamer⁵⁴,
 A. Hamilton^{145a}, G.N. Hamity^{145c}, P.G. Hamnett⁴², L. Han^{33b}, K. Hanagaki¹¹⁸, K. Hanawa¹⁵⁵,
 M. Hance¹⁵, P. Hanke^{58a}, R. Hanna¹³⁶, J.B. Hansen³⁶, J.D. Hansen³⁶, M.C. Hansen²¹,
 P.H. Hansen³⁶, K. Hara¹⁶⁰, A.S. Hard¹⁷³, T. Harenberg¹⁷⁵, F. Hariri¹¹⁷, S. Harkusha⁹²,
 R.D. Harrington⁴⁶, P.F. Harrison¹⁷⁰, F. Hartjes¹⁰⁷, M. Hasegawa⁶⁷, S. Hasegawa¹⁰³,
 Y. Hasegawa¹⁴⁰, A. Hasib¹¹³, S. Hassani¹³⁶, S. Haug¹⁷, R. Hauser⁹⁰, L. Hauswald⁴⁴,
 M. Havranek¹²⁷, C.M. Hawkes¹⁸, R.J. Hawkins³⁰, A.D. Hawkins⁸¹, T. Hayashi¹⁶⁰, D. Hayden⁹⁰,
 C.P. Hays¹²⁰, J.M. Hays⁷⁶, H.S. Hayward⁷⁴, S.J. Haywood¹³¹, S.J. Head¹⁸, T. Heck⁸³,
 V. Hedberg⁸¹, L. Heelan⁸, S. Heim¹²², T. Heim¹⁷⁵, B. Heinemann¹⁵, L. Heinrich¹¹⁰, J. Hejbal¹²⁷,
 L. Helary²², S. Hellman^{146a,146b}, D. Hellmich²¹, C. Hensens³⁰, J. Henderson¹²⁰,
 R.C.W. Henderson⁷², Y. Heng¹⁷³, C. Hengler⁴², A. Henrichs¹⁷⁶, A.M. Henriques Correia³⁰,
 S. Henrot-Versille¹¹⁷, G.H. Herbert¹⁶, Y. Hernández Jiménez¹⁶⁷, R. Herrberg-Schubert¹⁶,
 G. Herten⁴⁸, R. Hertenberger¹⁰⁰, L. Hervas³⁰, G.G. Hesketh⁷⁸, N.P. Hessey¹⁰⁷, J.W. Hetherly⁴⁰,
 R. Hickling⁷⁶, E. Higón-Rodríguez¹⁶⁷, E. Hill¹⁶⁹, J.C. Hill²⁸, K.H. Hiller⁴², S.J. Hillier¹⁸,
 I. Hinchliffe¹⁵, E. Hines¹²², R.R. Hinman¹⁵, M. Hirose¹⁵⁷, D. Hirschbuehl¹⁷⁵, J. Hobbs¹⁴⁸,
 N. Hod¹⁰⁷, M.C. Hodgkinson¹³⁹, P. Hodgson¹³⁹, A. Hoecker³⁰, M.R. Hoferkamp¹⁰⁵, F. Hoenig¹⁰⁰,
 M. Hohlfeld⁸³, D. Hohn²¹, T.R. Holmes¹⁵, M. Homann⁴³, T.M. Hong¹²⁵,
 L. Hooft van Huysduynen¹¹⁰, W.H. Hopkins¹¹⁶, Y. Horii¹⁰³, A.J. Horton¹⁴², J.-Y. Hostachy⁵⁵,
 S. Hou¹⁵¹, A. Hoummada^{135a}, J. Howard¹²⁰, J. Howarth⁴², M. Hrabovsky¹¹⁵, I. Hristova¹⁶,
 J. Hrivnac¹¹⁷, T. Hryn'ova⁵, A. Hrynevich⁹³, C. Hsu^{145c}, P.J. Hsu^{151,p}, S.-C. Hsu¹³⁸, D. Hu³⁵,
 Q. Hu^{33b}, X. Hu⁸⁹, Y. Huang⁴², Z. Hubacek³⁰, F. Hubaut⁸⁵, F. Huegging²¹, T.B. Huffman¹²⁰,
 E.W. Hughes³⁵, G. Hughes⁷², M. Huhtinen³⁰, T.A. Hülsing⁸³, N. Huseynov^{65,b}, J. Huston⁹⁰,

J. Huth⁵⁷, G. Iacobucci⁴⁹, G. Iakovidis²⁵, I. Ibragimov¹⁴¹, L. Iconomidou-Fayard¹¹⁷, E. Ideal¹⁷⁶, Z. Idrissi^{135e}, P. Iengo³⁰, O. Igonkina¹⁰⁷, T. Iizawa¹⁷¹, Y. Ikegami⁶⁶, K. Ikematsu¹⁴¹, M. Ikeno⁶⁶, Y. Ilchenko^{31,q}, D. Iliadis¹⁵⁴, N. Ilic¹⁴³, Y. Inamaru⁶⁷, T. Ince¹⁰¹, P. Ioannou⁹, M. Iodice^{134a}, K. Iordanidou³⁵, V. Ippolito⁵⁷, A. Irlles Quiles¹⁶⁷, C. Isaksson¹⁶⁶, M. Ishino⁶⁸, M. Ishitsuka¹⁵⁷, R. Ishmukhametov¹¹¹, C. Issever¹²⁰, S. Istin^{19a}, J.M. Iturbe Ponce⁸⁴, R. Iuppa^{133a,133b}, J. Ivarsson⁸¹, W. Iwanski³⁹, H. Iwasaki⁶⁶, J.M. Izen⁴¹, V. Izzo^{104a}, S. Jabbar³, B. Jackson¹²², M. Jackson⁷⁴, P. Jackson¹, M.R. Jaekel³⁰, V. Jain², K. Jakobs⁴⁸, S. Jakobsen³⁰, T. Jakoubek¹²⁷, J. Jakubek¹²⁸, D.O. Jamin¹⁵¹, D.K. Jana⁷⁹, E. Jansen⁷⁸, R.W. Jansky⁶², J. Janssen²¹, M. Janus¹⁷⁰, G. Jarlskog⁸¹, N. Javadov^{65,b}, T. Javurek⁴⁸, L. Jeanty¹⁵, J. Jejelava^{51a,r}, G.-Y. Jeng¹⁵⁰, D. Jennens⁸⁸, P. Jenni^{48,s}, J. Jentzsch⁴³, C. Jeske¹⁷⁰, S. Jézéquel⁵, H. Ji¹⁷³, J. Jia¹⁴⁸, Y. Jiang^{33b}, S. Jiggins⁷⁸, J. Jimenez Pena¹⁶⁷, S. Jin^{33a}, A. Jinaru^{26a}, O. Jinnouchi¹⁵⁷, M.D. Joergensen³⁶, P. Johansson¹³⁹, K.A. Johns⁷, K. Jon-And^{146a,146b}, G. Jones¹⁷⁰, R.W.L. Jones⁷², T.J. Jones⁷⁴, J. Jongmanns^{58a}, P.M. Jorge^{126a,126b}, K.D. Joshi⁸⁴, J. Jovicevic^{159a}, X. Ju¹⁷³, C.A. Jung⁴³, P. Jussel⁶², A. Juste Rozas^{12,o}, M. Kaci¹⁶⁷, A. Kaczmarek³⁹, M. Kado¹¹⁷, H. Kagan¹¹¹, M. Kagan¹⁴³, S.J. Kahn⁸⁵, E. Kajomovitz⁴⁵, C.W. Kalderon¹²⁰, S. Kama⁴⁰, A. Kamenshchikov¹³⁰, N. Kanaya¹⁵⁵, M. Kaneda³⁰, S. Kaneti²⁸, V.A. Kantserov⁹⁸, J. Kanzaki⁶⁶, B. Kaplan¹¹⁰, A. Kapliy³¹, D. Kar⁵³, K. Karakostas¹⁰, A. Karamaoun³, N. Karastathis^{10,107}, M.J. Kareem⁵⁴, M. Karnevskiy⁸³, S.N. Karpov⁶⁵, Z.M. Karpova⁶⁵, K. Karthik¹¹⁰, V. Kartvelishvili⁷², A.N. Karyukhin¹³⁰, L. Kashif¹⁷³, R.D. Kass¹¹¹, A. Kastanas¹⁴, Y. Kataoka¹⁵⁵, A. Katre⁴⁹, J. Katzy⁴², K. Kawagoe⁷⁰, T. Kawamoto¹⁵⁵, G. Kawamura⁵⁴, S. Kazama¹⁵⁵, V.F. Kazanin^{109,c}, M.Y. Kazarinov⁶⁵, R. Keeler¹⁶⁹, R. Kehoe⁴⁰, J.S. Keller⁴², J.J. Kempster⁷⁷, H. Keoshkerian⁸⁴, O. Kepka¹²⁷, B.P. Kerševan⁷⁵, S. Kersten¹⁷⁵, R.A. Keyes⁸⁷, F. Khalil-zada¹¹, H. Khandanyan^{146a,146b}, A. Khanov¹¹⁴, A.G. Kharlamov^{109,c}, T.J. Khoo²⁸, V. Khovanskiy⁹⁷, E. Khramov⁶⁵, J. Khubua^{51b,t}, H.Y. Kim⁸, H. Kim^{146a,146b}, S.H. Kim¹⁶⁰, Y. Kim³¹, N. Kimura¹⁵⁴, O.M. Kind¹⁶, B.T. King⁷⁴, M. King¹⁶⁷, S.B. King¹⁶⁸, J. Kirk¹³¹, A.E. Kiryunin¹⁰¹, T. Kishimoto⁶⁷, D. Kisielewska^{38a}, F. Kiss⁴⁸, K. Kiuchi¹⁶⁰, O. Kivernyk¹³⁶, E. Kladiva^{144b}, M.H. Klein³⁵, M. Klein⁷⁴, U. Klein⁷⁴, K. Kleinknecht⁸³, P. Klimek^{146a,146b}, A. Klimentov²⁵, R. Klingenberg⁴³, J.A. Klinger¹³⁹, T. Klioutchnikova³⁰, E.-E. Kluge^{58a}, P. Kluit¹⁰⁷, S. Kluth¹⁰¹, E. Kneringer⁶², E.B.F.G. Knoops⁸⁵, A. Knue⁵³, A. Kobayashi¹⁵⁵, D. Kobayashi¹⁵⁷, T. Kobayashi¹⁵⁵, M. Kobel⁴⁴, M. Kocian¹⁴³, P. Kodys¹²⁹, T. Koffas²⁹, E. Koffeman¹⁰⁷, L.A. Kogan¹²⁰, S. Kohlmann¹⁷⁵, Z. Kohout¹²⁸, T. Kohriki⁶⁶, T. Koi¹⁴³, H. Kolanoski¹⁶, I. Koletsou⁵, A.A. Komar^{96,*}, Y. Komori¹⁵⁵, T. Kondo⁶⁶, N. Kondrashova⁴², K. Köneke⁴⁸, A.C. König¹⁰⁶, S. König⁸³, T. Kono^{66,u}, R. Konoplich^{110,v}, N. Konstantinidis⁷⁸, R. Kopeliansky¹⁵², S. Koperny^{38a}, L. Köpke⁸³, A.K. Kopp⁴⁸, K. Korcyl³⁹, K. Kordas¹⁵⁴, A. Korn⁷⁸, A.A. Korol^{109,c}, I. Korolkov¹², E.V. Korolkova¹³⁹, O. Kortner¹⁰¹, S. Kortner¹⁰¹, T. Kosek¹²⁹, V.V. Kostyukhin²¹, V.M. Kotov⁶⁵, A. Kotwal⁴⁵, A. Kourkouveli-Charalampidi¹⁵⁴, C. Kourkouvelis⁹, V. Kouskoura²⁵, A. Koutsman^{159a}, R. Kowalewski¹⁶⁹, T.Z. Kowalski^{38a}, W. Kozanecki¹³⁶, A.S. Kozhin¹³⁰, V.A. Kramarenko⁹⁹, G. Kramberger⁷⁵, D. Krasnopevtsev⁹⁸, M.W. Krasny⁸⁰, A. Krasznahorkay³⁰, J.K. Kraus²¹, A. Kravchenko²⁵, S. Kreiss¹¹⁰, M. Kretz^{58c}, J. Kretzschmar⁷⁴, K. Kreutzfeldt⁵², P. Krieger¹⁵⁸, K. Krizka³¹, K. Kroeninger⁴³, H. Kroha¹⁰¹, J. Kroll¹²², J. Kroseberg²¹, J. Krstic¹³, U. Kruchonak⁶⁵, H. Krüger²¹, N. Krumnack⁶⁴, Z.V. Krumshteyn⁶⁵, A. Kruse¹⁷³, M.C. Kruse⁴⁵, M. Kruskal²², T. Kubota⁸⁸, H. Kucuk⁷⁸, S. Kудay^{4c}, S. Kuehn⁴⁸, A. Kugel^{58c}, F. Kuger¹⁷⁴, A. Kuhl¹³⁷, T. Kuhl⁴², V. Kukhtin⁶⁵, Y. Kulchitsky⁹², S. Kuleshov^{32b}, M. Kuna^{132a,132b}, T. Kunigo⁶⁸, A. Kupco¹²⁷, H. Kurashige⁶⁷, Y.A. Kurochkin⁹², R. Kurumida⁶⁷, V. Kus¹²⁷, E.S. Kuwertz¹⁶⁹, M. Kuze¹⁵⁷, J. Kvita¹¹⁵, T. Kwan¹⁶⁹, D. Kyriazopoulos¹³⁹, A. La Rosa⁴⁹, J.L. La Rosa Navarro^{24d}, L. La Rotonda^{37a,37b}, C. Lacasta¹⁶⁷, F. Lacava^{132a,132b}, J. Lacey²⁹, H. Lacker¹⁶, D. Lacour⁸⁰, V.R. Lacuesta¹⁶⁷, E. Ladygin⁶⁵, R. Lafaye⁵, B. Laforge⁸⁰, T. Lagouri¹⁷⁶, S. Lai⁴⁸, L. Lambourne⁷⁸, S. Lammers⁶¹, C.L. Lampen⁷, W. Lampl⁷, E. Lançon¹³⁶, U. Landgraf⁴⁸, M.P.J. Landon⁷⁶, V.S. Lang^{58a},

J.C. Lange¹², A.J. Lankford¹⁶³, F. Lanni²⁵, K. Lantzsich³⁰, S. Laplace⁸⁰, C. Lapoire³⁰,
 J.F. Laporte¹³⁶, T. Lari^{91a}, F. Lasagni Manghi^{20a,20b}, M. Lassnig³⁰, P. Laurelli⁴⁷, W. Lavrijsen¹⁵,
 A.T. Law¹³⁷, P. Laycock⁷⁴, T. Lazovich⁵⁷, O. Le Dortz⁸⁰, E. Le Guirriec⁸⁵, E. Le Menedeu¹²,
 M. LeBlanc¹⁶⁹, T. LeCompte⁶, F. Ledroit-Guillon⁵⁵, C.A. Lee^{145b}, S.C. Lee¹⁵¹, L. Lee¹,
 G. Lefebvre⁸⁰, M. Lefebvre¹⁶⁹, F. Legger¹⁰⁰, C. Leggett¹⁵, A. Lehan⁷⁴, G. Lehmann Miotto³⁰,
 X. Lei⁷, W.A. Leight²⁹, A. Leisos¹⁵⁴, A.G. Leister¹⁷⁶, M.A.L. Leite^{24d}, R. Leitner¹²⁹,
 D. Lellouch¹⁷², B. Lemmer⁵⁴, K.J.C. Leney⁷⁸, T. Lenz²¹, B. Lenzi³⁰, R. Leone⁷, S. Leone^{124a,124b},
 C. Leonidopoulos⁴⁶, S. Leontsinis¹⁰, C. Leroy⁹⁵, C.G. Lester²⁸, M. Levchenko¹²³, J. Levêque⁵,
 D. Levin⁸⁹, L.J. Levinson¹⁷², M. Levy¹⁸, A. Lewis¹²⁰, A.M. Leyko²¹, M. Leyton⁴¹, B. Li^{33b,w},
 H. Li¹⁴⁸, H.L. Li³¹, L. Li⁴⁵, L. Li^{33e}, S. Li⁴⁵, Y. Li^{33c,x}, Z. Liang¹³⁷, H. Liao³⁴, B. Liberti^{133a},
 A. Liblong¹⁵⁸, P. Lichard³⁰, K. Lie¹⁶⁵, J. Liebal²¹, W. Liebig¹⁴, C. Limbach²¹, A. Limosani¹⁵⁰,
 S.C. Lin^{151,y}, T.H. Lin⁸³, F. Linde¹⁰⁷, B.E. Lindquist¹⁴⁸, J.T. Linnemann⁹⁰, E. Lipeles¹²²,
 A. Lipniacka¹⁴, M. Lisovyi^{58b}, T.M. Liss¹⁶⁵, D. Lissauer²⁵, A. Lister¹⁶⁸, A.M. Litke¹³⁷,
 B. Liu^{151,z}, D. Liu¹⁵¹, H. Liu⁸⁹, J. Liu⁸⁵, J.B. Liu^{33b}, K. Liu⁸⁵, L. Liu¹⁶⁵, M. Liu⁴⁵, M. Liu^{33b},
 Y. Liu^{33b}, M. Livan^{121a,121b}, A. Lleres⁵⁵, J. Llorente Merino⁸², S.L. Lloyd⁷⁶, F. Lo Sterzo¹⁵¹,
 E. Lobodzinska⁴², P. Loch⁷, W.S. Lockman¹³⁷, F.K. Loebinger⁸⁴, A.E. Loevschall-Jensen³⁶,
 A. Loginov¹⁷⁶, T. Lohse¹⁶, K. Lohwasser⁴², M. Lokajicek¹²⁷, B.A. Long²², J.D. Long⁸⁹,
 R.E. Long⁷², K.A. Looper¹¹¹, L. Lopes^{126a}, D. Lopez Mateos⁵⁷, B. Lopez Paredes¹³⁹,
 I. Lopez Paz¹², J. Lorenz¹⁰⁰, N. Lorenzo Martinez⁶¹, M. Losada¹⁶², P. Loscutoff¹⁵, P.J. Lösel¹⁰⁰,
 X. Lou^{33a}, A. Lounis¹¹⁷, J. Love⁶, P.A. Love⁷², N. Lu⁸⁹, H.J. Lubatti¹³⁸, C. Luci^{132a,132b},
 A. Lucotte⁵⁵, F. Luehring⁶¹, W. Lukas⁶², L. Luminari^{132a}, O. Lundberg^{146a,146b},
 B. Lund-Jensen¹⁴⁷, D. Lynn²⁵, R. Lysak¹²⁷, E. Lytken⁸¹, H. Ma²⁵, L.L. Ma^{33d}, G. Maccarrone⁴⁷,
 A. Macchiolo¹⁰¹, C.M. Macdonald¹³⁹, J. Machado Miguens^{122,126b}, D. Macina³⁰, D. Madaffari⁸⁵,
 R. Madar³⁴, H.J. Maddocks⁷², W.F. Mader⁴⁴, A. Madsen¹⁶⁶, S. Maeland¹⁴, T. Maeno²⁵,
 A. Maevskiy⁹⁹, E. Magradze⁵⁴, K. Mahboubi⁴⁸, J. Mahlstedt¹⁰⁷, C. Maiani¹³⁶, C. Maidantchik^{24a},
 A.A. Maier¹⁰¹, T. Maier¹⁰⁰, A. Maio^{126a,126b,126d}, S. Majewski¹¹⁶, Y. Makida⁶⁶, N. Makovec¹¹⁷,
 B. Malaescu⁸⁰, Pa. Malecki³⁹, V.P. Maleev¹²³, F. Malek⁵⁵, U. Mallik⁶³, D. Malon⁶, C. Malone¹⁴³,
 S. Maltezos¹⁰, V.M. Malyshev¹⁰⁹, S. Malyukov³⁰, J. Mamuzic⁴², G. Mancini⁴⁷, B. Mandelli³⁰,
 L. Mandelli^{91a}, I. Mandić⁷⁵, R. Mandrysch⁶³, J. Maneira^{126a,126b}, A. Manfredini¹⁰¹,
 L. Manhaes de Andrade Filho^{24b}, J. Manjarres Ramos^{159b}, A. Mann¹⁰⁰, P.M. Manning¹³⁷,
 A. Manousakis-Katsikakis⁹, B. Mansoulie¹³⁶, R. Mantifel⁸⁷, M. Mantoani⁵⁴, L. Mapelli³⁰,
 L. March^{145c}, G. Marchiori⁸⁰, M. Marcisovsky¹²⁷, C.P. Marino¹⁶⁹, M. Marjanovic¹³,
 D.E. Marley⁸⁹, F. Marroquim^{24a}, S.P. Marsden⁸⁴, Z. Marshall¹⁵, L.F. Marti¹⁷, S. Marti-Garcia¹⁶⁷,
 B. Martin⁹⁰, T.A. Martin¹⁷⁰, V.J. Martin⁴⁶, B. Martin dit Latour¹⁴, M. Martinez^{12,o},
 S. Martin-Haugh¹³¹, V.S. Martoiu^{26a}, A.C. Martyniuk⁷⁸, M. Marx¹³⁸, F. Marzano^{132a},
 A. Marzin³⁰, L. Masetti⁸³, T. Mashimo¹⁵⁵, R. Mashinistov⁹⁶, J. Masik⁸⁴, A.L. Maslennikov^{109,c},
 I. Massa^{20a,20b}, L. Massa^{20a,20b}, N. Massol⁵, P. Mastrandrea¹⁴⁸, A. Mastroberardino^{37a,37b},
 T. Masubuchi¹⁵⁵, P. Mättig¹⁷⁵, J. Mattmann⁸³, J. Maurer^{26a}, S.J. Maxfield⁷⁴, D.A. Maximov^{109,c},
 R. Mazini¹⁵¹, S.M. Mazza^{91a,91b}, L. Mazzaferro^{133a,133b}, G. Mc Goldrick¹⁵⁸, S.P. Mc Kee⁸⁹,
 A. McCarn⁸⁹, R.L. McCarthy¹⁴⁸, T.G. McCarthy²⁹, N.A. McCubbin¹³¹, K.W. McFarlane^{56,*},
 J.A. Mcfayden⁷⁸, G. Mchedlidze⁵⁴, S.J. McMahon¹³¹, R.A. McPherson^{169,k}, M. Medinnis⁴²,
 S. Meehan^{145a}, S. Mehlhase¹⁰⁰, A. Mehta⁷⁴, K. Meier^{58a}, C. Meineck¹⁰⁰, B. Meirose⁴¹,
 B.R. Mellado Garcia^{145c}, F. Meloni¹⁷, A. Mengarelli^{20a,20b}, S. Menke¹⁰¹, E. Meoni¹⁶¹,
 K.M. Mercurio⁵⁷, S. Mergelmeyer²¹, P. Mermod⁴⁹, L. Merola^{104a,104b}, C. Meroni^{91a},
 F.S. Merritt³¹, A. Messina^{132a,132b}, J. Metcalfe²⁵, A.S. Mete¹⁶³, C. Meyer⁸³, C. Meyer¹²²,
 J-P. Meyer¹³⁶, J. Meyer¹⁰⁷, R.P. Middleton¹³¹, S. Miglioranzi^{164a,164c}, L. Mijović²¹,
 G. Mikenberg¹⁷², M. Mikesikova¹²⁷, M. Mikuž⁷⁵, M. Milesi⁸⁸, A. Milic³⁰, D.W. Miller³¹,
 C. Mills⁴⁶, A. Milov¹⁷², D.A. Milstead^{146a,146b}, A.A. Minaenko¹³⁰, Y. Minami¹⁵⁵,
 I.A. Minashvili⁶⁵, A.I. Mincer¹¹⁰, B. Mindur^{38a}, M. Mineev⁶⁵, Y. Ming¹⁷³, L.M. Mir¹²,

T. Mitani¹⁷¹, J. Mitrevski¹⁰⁰, V.A. Mitsou¹⁶⁷, A. Miucci⁴⁹, P.S. Miyagawa¹³⁹, J.U. Mjörnmark⁸¹, T. Moa^{146a,146b}, K. Mochizuki⁸⁵, S. Mohapatra³⁵, W. Mohr⁴⁸, S. Molander^{146a,146b}, R. Moles-Valls¹⁶⁷, K. Mönig⁴², C. Monini⁵⁵, J. Monk³⁶, E. Monnier⁸⁵, J. Montejo Berlingen¹², F. Monticelli⁷¹, S. Monzani^{132a,132b}, R.W. Moore³, N. Morange¹¹⁷, D. Moreno¹⁶², M. Moreno Llácer⁵⁴, P. Morettini^{50a}, M. Morgenstern⁴⁴, M. Morii⁵⁷, M. Morinaga¹⁵⁵, V. Morisbak¹¹⁹, S. Moritz⁸³, A.K. Morley¹⁴⁷, G. Mornacchi³⁰, J.D. Morris⁷⁶, S.S. Mortensen³⁶, A. Morton⁵³, L. Morvaj¹⁰³, M. Mosidze^{51b}, J. Moss¹¹¹, K. Motohashi¹⁵⁷, R. Mount¹⁴³, E. Mountricha²⁵, S.V. Mouraviev^{96,*}, E.J.W. Moyses⁸⁶, S. Muanza⁸⁵, R.D. Mudd¹⁸, F. Mueller¹⁰¹, J. Mueller¹²⁵, K. Mueller²¹, R.S.P. Mueller¹⁰⁰, T. Mueller²⁸, D. Muenstermann⁴⁹, P. Mullen⁵³, G.A. Mullier¹⁷, Y. Munwes¹⁵³, J.A. Murillo Quijada¹⁸, W.J. Murray^{170,131}, H. Musheghyan⁵⁴, E. Musto¹⁵², A.G. Myagkov^{130,aa}, M. Myska¹²⁸, O. Nackenhorst⁵⁴, J. Nadal⁵⁴, K. Nagai¹²⁰, R. Nagai¹⁵⁷, Y. Nagai⁸⁵, K. Nagano⁶⁶, A. Nagarkar¹¹¹, Y. Nagasaka⁵⁹, K. Nagata¹⁶⁰, M. Nagel¹⁰¹, E. Nagy⁸⁵, A.M. Nairz³⁰, Y. Nakahama³⁰, K. Nakamura⁶⁶, T. Nakamura¹⁵⁵, I. Nakano¹¹², H. Namasivayam⁴¹, R.F. Naranjo Garcia⁴², R. Narayan³¹, T. Naumann⁴², G. Navarro¹⁶², R. Nayyar⁷, H.A. Neal⁸⁹, P.Yu. Nechaeva⁹⁶, T.J. Neep⁸⁴, P.D. Nef¹⁴³, A. Negri^{121a,121b}, M. Negrini^{20a}, S. Nektarijevic¹⁰⁶, C. Nellist¹¹⁷, A. Nelson¹⁶³, S. Nemecek¹²⁷, P. Nemethy¹¹⁰, A.A. Nepomuceno^{24a}, M. Nessi^{30,ab}, M.S. Neubauer¹⁶⁵, M. Neumann¹⁷⁵, R.M. Neves¹¹⁰, P. Nevski²⁵, P.R. Newman¹⁸, D.H. Nguyen⁶, R.B. Nickerson¹²⁰, R. Nicolaidou¹³⁶, B. Nicquevert³⁰, J. Nielsen¹³⁷, N. Nikiforou³⁵, A. Nikiforov¹⁶, V. Nikolaenko^{130,aa}, I. Nikolic-Audit⁸⁰, K. Nikolopoulos¹⁸, J.K. Nilsen¹¹⁹, P. Nilsson²⁵, Y. Ninomiya¹⁵⁵, A. Nisati^{132a}, R. Nisius¹⁰¹, T. Nobe¹⁵⁷, M. Nomachi¹¹⁸, I. Nomidis²⁹, T. Nooney⁷⁶, S. Norberg¹¹³, M. Nordberg³⁰, O. Novgorodova⁴⁴, S. Nowak¹⁰¹, M. Nozaki⁶⁶, L. Nozka¹¹⁵, K. Ntekas¹⁰, G. Nunes Hanninger⁸⁸, T. Nunnemann¹⁰⁰, E. Nurse⁷⁸, F. Nuti⁸⁸, B.J. O'Brien⁴⁶, F. O'grady⁷, D.C. O'Neil¹⁴², V. O'Shea⁵³, F.G. Oakham^{29,d}, H. Oberlack¹⁰¹, T. Obermann²¹, J. Ocariz⁸⁰, A. Ochi⁶⁷, I. Ochoa⁷⁸, J.P. Ochoa-Ricoux^{32a}, S. Oda⁷⁰, S. Odaka⁶⁶, H. Ogren⁶¹, A. Oh⁸⁴, S.H. Oh⁴⁵, C.C. Ohm¹⁵, H. Ohman¹⁶⁶, H. Oide³⁰, W. Okamura¹¹⁸, H. Okawa¹⁶⁰, Y. Okumura³¹, T. Okuyama¹⁵⁵, A. Olariu^{26a}, S.A. Olivares Pino⁴⁶, D. Oliveira Damazio²⁵, E. Oliver Garcia¹⁶⁷, A. Olszewski³⁹, J. Olszowska³⁹, A. Onofre^{126a,126e}, P.U.E. Onyisi^{31,q}, C.J. Oram^{159a}, M.J. Oreglia³¹, Y. Oren¹⁵³, D. Orestano^{134a,134b}, N. Orlando¹⁵⁴, C. Oropeza Barrera⁵³, R.S. Orr¹⁵⁸, B. Osculati^{50a,50b}, R. Ospanov⁸⁴, G. Otero y Garzon²⁷, H. Otono⁷⁰, M. Ouchrif^{135d}, E.A. Ouellette¹⁶⁹, F. Ould-Saada¹¹⁹, A. Ouraou¹³⁶, K.P. Oussoren¹⁰⁷, Q. Ouyang^{33a}, A. Ovcharova¹⁵, M. Owen⁵³, R.E. Owen¹⁸, V.E. Ozcan^{19a}, N. Ozturk⁸, K. Pachal¹⁴², A. Pacheco Pages¹², C. Padilla Aranda¹², M. Pagáčová⁴⁸, S. Pagan Griso¹⁵, E. Paganis¹³⁹, C. Pahl¹⁰¹, F. Paige²⁵, P. Pais⁸⁶, K. Pajchel¹¹⁹, G. Palacino^{159b}, S. Palestini³⁰, M. Palka^{38b}, D. Pallin³⁴, A. Palma^{126a,126b}, Y.B. Pan¹⁷³, E. Panagiotopoulou¹⁰, C.E. Pandini⁸⁰, J.G. Panduro Vazquez⁷⁷, P. Pani^{146a,146b}, S. Panitkin²⁵, D. Pantea^{26a}, L. Paolozzi⁴⁹, Th.D. Papadopoulou¹⁰, K. Papageorgiou¹⁵⁴, A. Paramonov⁶, D. Paredes Hernandez¹⁵⁴, M.A. Parker²⁸, K.A. Parker¹³⁹, F. Parodi^{50a,50b}, J.A. Parsons³⁵, U. Parzefall⁴⁸, E. Pasqualucci^{132a}, S. Passaggio^{50a}, F. Pastore^{134a,134b,*}, Fr. Pastore⁷⁷, G. Pásztor²⁹, S. Pataraja¹⁷⁵, N.D. Patel¹⁵⁰, J.R. Pater⁸⁴, T. Pauly³⁰, J. Pearce¹⁶⁹, B. Pearson¹¹³, L.E. Pedersen³⁶, M. Pedersen¹¹⁹, S. Pedraza Lopez¹⁶⁷, R. Pedro^{126a,126b}, S.V. Peleganchuk^{109,c}, D. Pelikan¹⁶⁶, H. Peng^{33b}, B. Penning³¹, J. Penwell⁶¹, D.V. Perepelitsa²⁵, E. Perez Codina^{159a}, M.T. Pérez García-Estañ¹⁶⁷, L. Perini^{91a,91b}, H. Pernegger³⁰, S. Perrella^{104a,104b}, R. Peschke⁴², V.D. Peshekhonov⁶⁵, K. Peters³⁰, R.F.Y. Peters⁸⁴, B.A. Petersen³⁰, T.C. Petersen³⁶, E. Petit⁴², A. Petridis^{146a,146b}, C. Petridou¹⁵⁴, E. Petrolo^{132a}, F. Petrucci^{134a,134b}, N.E. Pettersson¹⁵⁷, R. Pezoa^{32b}, P.W. Phillips¹³¹, G. Piacquadio¹⁴³, E. Pianori¹⁷⁰, A. Picazio⁴⁹, E. Piccaro⁷⁶, M. Piccinini^{20a,20b}, M.A. Pickering¹²⁰, R. Piegai²⁷, D.T. Pignotti¹¹¹, J.E. Pilcher³¹, A.D. Pilkington⁸⁴, J. Pina^{126a,126b,126d}, M. Pinamonti^{164a,164c,ac}, J.L. Pinfold³, A. Pingel³⁶, B. Pinto^{126a}, S. Pires⁸⁰, H. Pirumov⁴², M. Pitt¹⁷², C. Pizio^{91a,91b}, L. Plazak^{144a}, M.-A. Pleier²⁵,

V. Pleskot¹²⁹, E. Plotnikova⁶⁵, P. Plucinski^{146a,146b}, D. Pluth⁶⁴, R. Poettgen^{146a,146b},
L. Poggioli¹¹⁷, D. Pohl²¹, G. Polesello^{121a}, A. Poley⁴², A. Policicchio^{37a,37b}, R. Polifka¹⁵⁸,
A. Polini^{20a}, C.S. Pollard⁵³, V. Polychronakos²⁵, K. Pommès³⁰, L. Pontecorvo^{132a}, B.G. Pope⁹⁰,
G.A. Popeneciu^{26b}, D.S. Popovic¹³, A. Poppleton³⁰, S. Pospisil¹²⁸, K. Potamianos¹⁵,
I.N. Potrap⁶⁵, C.J. Potter¹⁴⁹, C.T. Potter¹¹⁶, G. Poulard³⁰, J. Poveda³⁰, V. Pozdnyakov⁶⁵,
P. Pralavorio⁸⁵, A. Pranko¹⁵, S. Prasad³⁰, S. Prell⁶⁴, D. Price⁸⁴, L.E. Price⁶, M. Primavera^{73a},
S. Prince⁸⁷, M. Proissl⁴⁶, K. Prokofiev^{60c}, F. Prokoshin^{32b}, E. Protopapadaki¹³⁶,
S. Protopopescu²⁵, J. Proudfoot⁶, M. Przybycien^{38a}, E. Ptacek¹¹⁶, D. Puddu^{134a,134b},
E. Pueschel⁸⁶, D. Puldon¹⁴⁸, M. Purohit^{25,ad}, P. Puzo¹¹⁷, J. Qian⁸⁹, G. Qin⁵³, Y. Qin⁸⁴,
A. Quadt⁵⁴, D.R. Quarrie¹⁵, W.B. Quayle^{164a,164b}, M. Queitsch-Maitland⁸⁴, D. Quilty⁵³,
S. Raddum¹¹⁹, V. Radeka²⁵, V. Radescu⁴², S.K. Radhakrishnan¹⁴⁸, P. Radloff¹¹⁶, P. Rados⁸⁸,
F. Ragusa^{91a,91b}, G. Rahal¹⁷⁸, S. Rajagopalan²⁵, M. Rammensee³⁰, C. Rangel-Smith¹⁶⁶,
F. Rauscher¹⁰⁰, S. Rave⁸³, T. Ravenscroft⁵³, M. Raymond³⁰, A.L. Read¹¹⁹, N.P. Readioff⁷⁴,
D.M. Rebutzi^{121a,121b}, A. Redelbach¹⁷⁴, G. Redlinger²⁵, R. Reece¹³⁷, K. Reeves⁴¹, L. Rehnisch¹⁶,
H. Reisin²⁷, M. Relich¹⁶³, C. Rembser³⁰, H. Ren^{33a}, A. Renaud¹¹⁷, M. Rescigno^{132a},
S. Resconi^{91a}, O.L. Rezanova^{109,c}, P. Reznicek¹²⁹, R. Rezvani⁹⁵, R. Richter¹⁰¹, S. Richter⁷⁸,
E. Richter-Was^{38b}, O. Ricken²¹, M. Ridel⁸⁰, P. Rieck¹⁶, C.J. Riegel¹⁷⁵, J. Rieger⁵⁴,
M. Rijssenbeek¹⁴⁸, A. Rimoldi^{121a,121b}, L. Rinaldi^{20a}, B. Ristić⁴⁹, E. Ritsch³⁰, I. Riu¹²,
F. Rizatdinova¹¹⁴, E. Rizvi⁷⁶, S.H. Robertson^{87,k}, A. Robichaud-Veronneau⁸⁷, D. Robinson²⁸,
J.E.M. Robinson⁸⁴, A. Robson⁵³, C. Roda^{124a,124b}, S. Roe³⁰, O. Røhne¹¹⁹, S. Rolli¹⁶¹,
A. Romaniouk⁹⁸, M. Romano^{20a,20b}, S.M. Romano Saez³⁴, E. Romero Adam¹⁶⁷, N. Rompotis¹³⁸,
M. Ronzani⁴⁸, L. Roos⁸⁰, E. Ros¹⁶⁷, S. Rosati^{132a}, K. Rosbach⁴⁸, P. Rose¹³⁷, P.L. Rosendahl¹⁴,
O. Rosenthal¹⁴¹, V. Rossetti^{146a,146b}, E. Rossi^{104a,104b}, L.P. Rossi^{50a}, R. Rosten¹³⁸, M. Rotaru^{26a},
I. Roth¹⁷², J. Rothberg¹³⁸, D. Rousseau¹¹⁷, C.R. Royon¹³⁶, A. Rozanov⁸⁵, Y. Rozen¹⁵²,
X. Ruan^{145c}, F. Rubbo¹⁴³, I. Rubinskiy⁴², V.I. Rud⁹⁹, C. Rudolph⁴⁴, M.S. Rudolph¹⁵⁸, F. Rühr⁴⁸,
A. Ruiz-Martinez³⁰, Z. Rurikova⁴⁸, N.A. Rusakovich⁶⁵, A. Ruschke¹⁰⁰, H.L. Russell¹³⁸,
J.P. Rutherford⁷, N. Ruthmann⁴⁸, Y.F. Ryabov¹²³, M. Rybar¹²⁹, G. Rybkin¹¹⁷, N.C. Ryder¹²⁰,
A.F. Saavedra¹⁵⁰, G. Sabato¹⁰⁷, S. Sacerdoti²⁷, A. Saddique³, H.F.W. Sadrozinski¹³⁷,
R. Sadykov⁶⁵, F. Safai Tehrani^{132a}, M. Saimpert¹³⁶, H. Sakamoto¹⁵⁵, Y. Sakurai¹⁷¹,
G. Salamanna^{134a,134b}, A. Salamon^{133a}, M. Saleem¹¹³, D. Salek¹⁰⁷, P.H. Sales De Bruin¹³⁸,
D. Salihagic¹⁰¹, A. Salnikov¹⁴³, J. Salt¹⁶⁷, D. Salvatore^{37a,37b}, F. Salvatore¹⁴⁹, A. Salvucci¹⁰⁶,
A. Salzburger³⁰, D. Sampsonidis¹⁵⁴, A. Sanchez^{104a,104b}, J. Sánchez¹⁶⁷, V. Sanchez Martinez¹⁶⁷,
H. Sandaker¹⁴, R.L. Sandbach⁷⁶, H.G. Sander⁸³, M.P. Sanders¹⁰⁰, M. Sandhoff¹⁷⁵, C. Sandoval¹⁶²,
R. Sandstroem¹⁰¹, D.P.C. Sankey¹³¹, M. Sannino^{50a,50b}, A. Sansoni⁴⁷, C. Santoni³⁴,
R. Santonicio^{133a,133b}, H. Santos^{126a}, I. Santoyo Castillo¹⁴⁹, K. Sapp¹²⁵, A. Saponov⁶⁵,
J.G. Saraiva^{126a,126d}, B. Sarrazin²¹, O. Sasaki⁶⁶, Y. Sasaki¹⁵⁵, K. Sato¹⁶⁰, G. Sauvage^{5,*},
E. Sauvan⁵, G. Savage⁷⁷, P. Savard^{158,d}, C. Sawyer¹³¹, L. Sawyer^{79,n}, J. Saxon³¹, C. Sbarra^{20a},
A. Sbrizzi^{20a,20b}, T. Scanlon⁷⁸, D.A. Scannicchio¹⁶³, M. Scarcella¹⁵⁰, V. Scarfone^{37a,37b},
J. Schaarschmidt¹⁷², P. Schacht¹⁰¹, D. Schaefer³⁰, R. Schaefer⁴², J. Schaeffer⁸³, S. Schaepe²¹,
S. Schaetzel^{58b}, U. Schäfer⁸³, A.C. Schaffer¹¹⁷, D. Schaile¹⁰⁰, R.D. Schamberger¹⁴⁸, V. Scharf^{58a},
V.A. Schegelsky¹²³, D. Scheirich¹²⁹, M. Schernau¹⁶³, C. Schiavi^{50a,50b}, C. Schillo⁴⁸,
M. Schioppa^{37a,37b}, S. Schlenker³⁰, E. Schmidt⁴⁸, K. Schmieden³⁰, C. Schmitt⁸³, S. Schmitt^{58b},
S. Schmitt⁴², B. Schneider^{159a}, Y.J. Schnellbach⁷⁴, U. Schnoor⁴⁴, L. Schoeffel¹³⁶, A. Schoening^{58b},
B.D. Schoenrock⁹⁰, E. Schopf²¹, A.L.S. Schorlemmer⁵⁴, M. Schott⁸³, D. Schouten^{159a},
J. Schovancova⁸, S. Schramm¹⁵⁸, M. Schreyer¹⁷⁴, C. Schroeder⁸³, N. Schuh⁸³, M.J. Schultens²¹,
H.-C. Schultz-Coulon^{58a}, H. Schulz¹⁶, M. Schumacher⁴⁸, B.A. Schumm¹³⁷, Ph. Schune¹³⁶,
C. Schwanenberger⁸⁴, A. Schwartzman¹⁴³, T.A. Schwarz⁸⁹, Ph. Schwegler¹⁰¹, Ph. Schwemling¹³⁶,
R. Schwienhorst⁹⁰, J. Schwindling¹³⁶, T. Schwindt²¹, F.G. Sciacca¹⁷, E. Scifo¹¹⁷, G. Sciolla²³,
F. Scuri^{124a,124b}, F. Scutti²¹, J. Searcy⁸⁹, G. Sedov⁴², E. Sedykh¹²³, P. Seema²¹, S.C. Seidel¹⁰⁵,

A. Seiden¹³⁷, F. Seifert¹²⁸, J.M. Seixas^{24a}, G. Sekhniaidze^{104a}, K. Sekhon⁸⁹, S.J. Sekula⁴⁰,
 D.M. Seliverstov^{123,*}, N. Semprini-Cesari^{20a,20b}, C. Serfon³⁰, L. Serin¹¹⁷, L. Serkin^{164a,164b},
 T. Serre⁸⁵, M. Sessa^{134a,134b}, R. Seuster^{159a}, H. Severini¹¹³, T. Sfiligoj⁷⁵, F. Sforza³⁰, A. Sfyrla³⁰,
 E. Shabalina⁵⁴, M. Shamim¹¹⁶, L.Y. Shan^{33a}, R. Shang¹⁶⁵, J.T. Shank²², M. Shapiro¹⁵,
 P.B. Shatalov⁹⁷, K. Shaw^{164a,164b}, S.M. Shaw⁸⁴, A. Shcherbakova^{146a,146b}, C.Y. Shehu¹⁴⁹,
 P. Sherwood⁷⁸, L. Shi^{151,ae}, S. Shimizu⁶⁷, C.O. Shimmin¹⁶³, M. Shimojima¹⁰², M. Shiyakova⁶⁵,
 A. Shmeleva⁹⁶, D. Shoaleh Saadi⁹⁵, M.J. Shochet³¹, S. Shojaii^{91a,91b}, S. Shrestha¹¹¹, E. Shulga⁹⁸,
 M.A. Shupe⁷, S. Shushkevich⁴², P. Sicho¹²⁷, O. Sidiropoulou¹⁷⁴, D. Sidorov¹¹⁴, A. Sidoti^{20a,20b},
 F. Siegert⁴⁴, Dj. Sijacki¹³, J. Silva^{126a,126d}, Y. Silver¹⁵³, S.B. Silverstein^{146a}, V. Simak¹²⁸,
 O. Simard⁵, Lj. Simic¹³, S. Simion¹¹⁷, E. Simioni⁸³, B. Simmons⁷⁸, D. Simon³⁴,
 R. Simoniello^{91a,91b}, P. Sinervo¹⁵⁸, N.B. Sinev¹¹⁶, G. Siragusa¹⁷⁴, A.N. Sisakyan^{65,*},
 S.Yu. Sivoklov⁹⁹, J. Sjölin^{146a,146b}, T.B. Sjurjen¹⁴, M.B. Skinner⁷², H.P. Skottowe⁵⁷,
 P. Skubic¹¹³, M. Slater¹⁸, T. Slavicek¹²⁸, M. Slawinska¹⁰⁷, K. Sliwa¹⁶¹, V. Smakhtin¹⁷²,
 B.H. Smart⁴⁶, L. Smestad¹⁴, S.Yu. Smirnov⁹⁸, Y. Smirnov⁹⁸, L.N. Smirnova^{99,af}, O. Smirnova⁸¹,
 M.N.K. Smith³⁵, R.W. Smith³⁵, M. Smizanska⁷², K. Smolek¹²⁸, A.A. Snesarev⁹⁶, G. Snidero⁷⁶,
 S. Snyder²⁵, R. Sobie^{169,k}, F. Socher⁴⁴, A. Soffer¹⁵³, D.A. Soh^{151,ae}, C.A. Solans³⁰, M. Solar¹²⁸,
 J. Solc¹²⁸, E.Yu. Soldatov⁹⁸, U. Soldevila¹⁶⁷, A.A. Solodkov¹³⁰, A. Soloshenko⁶⁵,
 O.V. Solovyanov¹³⁰, V. Solovyev¹²³, P. Sommer⁴⁸, H.Y. Song^{33b}, N. Soni¹, A. Sood¹⁵,
 A. Sopczak¹²⁸, B. Sopko¹²⁸, V. Sopko¹²⁸, V. Sorin¹², D. Sosa^{58b}, M. Sosebee⁸,
 C.L. Sotiropoulou^{124a,124b}, R. Soualah^{164a,164c}, A.M. Soukharev^{109,c}, D. South⁴², B.C. Sowden⁷⁷,
 S. Spagnolo^{73a,73b}, M. Spalla^{124a,124b}, F. Spanò⁷⁷, W.R. Spearman⁵⁷, F. Spettel¹⁰¹, R. Spighi^{20a},
 G. Spigo³⁰, L.A. Spiller⁸⁸, M. Spousta¹²⁹, T. Spreitzer¹⁵⁸, R.D. St. Denis^{53,*}, S. Staerz⁴⁴,
 J. Stahlman¹²², R. Stamen^{58a}, S. Stamm¹⁶, E. Stanecka³⁹, C. Stanescu^{134a}, M. Stanescu-Bellu⁴²,
 M.M. Stanitzki⁴², S. Stapnes¹¹⁹, E.A. Starchenko¹³⁰, J. Stark⁵⁵, P. Staroba¹²⁷, P. Starovoitov⁴²,
 R. Staszewski³⁹, P. Stavina^{144a,*}, P. Steinberg²⁵, B. Stelzer¹⁴², H.J. Stelzer³⁰,
 O. Stelzer-Chilton^{159a}, H. Stenzel⁵², S. Stern¹⁰¹, G.A. Stewart⁵³, J.A. Stillings²¹,
 M.C. Stockton⁸⁷, M. Stoebe⁸⁷, G. Stoicea^{26a}, P. Stolte⁵⁴, S. Stonjek¹⁰¹, A.R. Stradling⁸,
 A. Straessner⁴⁴, M.E. Stramaglia¹⁷, J. Strandberg¹⁴⁷, S. Strandberg^{146a,146b}, A. Strandlie¹¹⁹,
 E. Strauss¹⁴³, M. Strauss¹¹³, P. Strizeneč^{144b}, R. Ströhmer¹⁷⁴, D.M. Strom¹¹⁶, R. Stroynowski⁴⁰,
 A. Strubig¹⁰⁶, S.A. Stucci¹⁷, B. Stugu¹⁴, N.A. Styles⁴², D. Su¹⁴³, J. Su¹²⁵, R. Subramaniam⁷⁹,
 A. Succurro¹², Y. Sugaya¹¹⁸, C. Suhr¹⁰⁸, M. Suk¹²⁸, V.V. Sulin⁹⁶, S. Sultansoy^{4d}, T. Sumida⁶⁸,
 S. Sun⁵⁷, X. Sun^{33a}, J.E. Sundermann⁴⁸, K. Suruliz¹⁴⁹, G. Susinno^{37a,37b}, M.R. Sutton¹⁴⁹,
 S. Suzuki⁶⁶, Y. Suzuki⁶⁶, M. Svatos¹²⁷, S. Swedish¹⁶⁸, M. Swiatlowski¹⁴³, I. Sykora^{144a},
 T. Sykora¹²⁹, D. Ta⁹⁰, C. Taccini^{134a,134b}, K. Tackmann⁴², J. Taenzer¹⁵⁸, A. Taffard¹⁶³,
 R. Tafirout^{159a}, N. Taiblum¹⁵³, H. Takai²⁵, R. Takashima⁶⁹, H. Takeda⁶⁷, T. Takeshita¹⁴⁰,
 Y. Takubo⁶⁶, M. Talby⁸⁵, A.A. Talyshev^{109,c}, J.Y.C. Tam¹⁷⁴, K.G. Tan⁸⁸, J. Tanaka¹⁵⁵,
 R. Tanaka¹¹⁷, S. Tanaka⁶⁶, B.B. Tannenwald¹¹¹, N. Tannoury²¹, S. Tapprogge⁸³, S. Tarem¹⁵²,
 F. Tarrade²⁹, G.F. Tartarelli^{91a}, P. Tas¹²⁹, M. Tasevsky¹²⁷, T. Tashiro⁶⁸, E. Tassi^{37a,37b},
 A. Tavares Delgado^{126a,126b}, Y. Tayalati^{135d}, F.E. Taylor⁹⁴, G.N. Taylor⁸⁸, W. Taylor^{159b},
 F.A. Teischinger³⁰, M. Teixeira Dias Castanheira⁷⁶, P. Teixeira-Dias⁷⁷, K.K. Temming⁴⁸,
 H. Ten Kate³⁰, P.K. Teng¹⁵¹, J.J. Teoh¹¹⁸, F. Tepel¹⁷⁵, S. Terada⁶⁶, K. Terashi¹⁵⁵, J. Terron⁸²,
 S. Terzo¹⁰¹, M. Testa⁴⁷, R.J. Teuscher^{158,k}, J. Therhaag²¹, T. Theveneaux-Pelzer³⁴,
 J.P. Thomas¹⁸, J. Thomas-Wilsker⁷⁷, E.N. Thompson³⁵, P.D. Thompson¹⁸, R.J. Thompson⁸⁴,
 A.S. Thompson⁵³, L.A. Thomsen¹⁷⁶, E. Thomson¹²², M. Thomson²⁸, R.P. Thun^{89,*},
 M.J. Tibbetts¹⁵, R.E. Ticse Torres⁸⁵, V.O. Tikhomirov^{96,ag}, Yu.A. Tikhonov^{109,c},
 S. Timoshenko⁹⁸, E. Tiouchichine⁸⁵, P. Tipton¹⁷⁶, S. Tisserant⁸⁵, T. Todorov^{5,*},
 S. Todorova-Nova¹²⁹, J. Tojo⁷⁰, S. Tokár^{144a}, K. Tokushuku⁶⁶, K. Tollefson⁹⁰, E. Tolley⁵⁷,
 L. Tomlinson⁸⁴, M. Tomoto¹⁰³, L. Tompkins^{143,ah}, K. Toms¹⁰⁵, E. Torrence¹¹⁶, H. Torres¹⁴²,
 E. Torró Pastor¹⁶⁷, J. Toth^{85,ai}, F. Touchard⁸⁵, D.R. Tovey¹³⁹, T. Trefzger¹⁷⁴, L. Tremblet³⁰,

A. Tricoli³⁰, I.M. Trigger^{159a}, S. Trincaz-Duvoid⁸⁰, M.F. Tripana¹², W. Trischuk¹⁵⁸, B. Trocmé⁵⁵,
 C. Troncon^{91a}, M. Trottier-McDonald¹⁵, M. Trovatelli¹⁶⁹, P. True⁹⁰, L. Truong^{164a,164c},
 M. Trzebinski³⁹, A. Trzupiek³⁹, C. Tsarouchas³⁰, J.C-L. Tseng¹²⁰, P.V. Tsiarashka⁹²,
 D. Tsionou¹⁵⁴, G. Tsipolitis¹⁰, N. Tsirintanis⁹, S. Tsiskaridze¹², V. Tsiskaridze⁴⁸,
 E.G. Tskhadadze^{51a}, I.I. Tsukerman⁹⁷, V. Tsulaia¹⁵, S. Tsuno⁶⁶, D. Tsybychev¹⁴⁸,
 A. Tudorache^{26a}, V. Tudorache^{26a}, A.N. Tuna¹²², S.A. Tuppuri^{20a,20b}, S. Turchikhin^{99,af},
 D. Turecek¹²⁸, R. Turra^{91a,91b}, A.J. Turvey⁴⁰, P.M. Tuts³⁵, A. Tykhonov⁴⁹, M. Tylmad^{146a,146b},
 M. Tyndel¹³¹, I. Ueda¹⁵⁵, R. Ueno²⁹, M. Ughetto^{146a,146b}, M. Ugland¹⁴, M. Uhlenbrock²¹,
 F. Ukegawa¹⁶⁰, G. Unal³⁰, A. Undrus²⁵, G. Unel¹⁶³, F.C. Ungaro⁴⁸, Y. Unno⁶⁶,
 C. Unverdorben¹⁰⁰, J. Urban^{144b}, P. Urquijo⁸⁸, P. Urrejola⁸³, G. Usai⁸, A. Usanova⁶²,
 L. Vacavant⁸⁵, V. Vacek¹²⁸, B. Vachon⁸⁷, C. Valderanis⁸³, N. Valencic¹⁰⁷, S. Valentinetti^{20a,20b},
 A. Valero¹⁶⁷, L. Valery¹², S. Valkar¹²⁹, E. Valladolid Gallego¹⁶⁷, S. Vallecorsa⁴⁹,
 J.A. Valls Ferrer¹⁶⁷, W. Van Den Wollenberg¹⁰⁷, P.C. Van Der Deijl¹⁰⁷, R. van der Geer¹⁰⁷,
 H. van der Graaf¹⁰⁷, R. Van Der Leeuw¹⁰⁷, N. van Eldik¹⁵², P. van Gemmeren⁶,
 J. Van Nieuwkoop¹⁴², I. van Vulpen¹⁰⁷, M.C. van Woerden³⁰, M. Vanadia^{132a,132b}, W. Vandelli³⁰,
 R. Vanguri¹²², A. Vaniachine⁶, F. Vannucci⁸⁰, G. Vardanyan¹⁷⁷, R. Vari^{132a}, E.W. Varnes⁷,
 T. Varol⁴⁰, D. Varouchas⁸⁰, A. Vartapetian⁸, K.E. Varvell¹⁵⁰, F. Vazeille³⁴,
 T. Vazquez Schroeder⁸⁷, J. Veatch⁷, L.M. Veloce¹⁵⁸, F. Veloso^{126a,126c}, T. Velz²¹,
 S. Veneziano^{132a}, A. Ventura^{73a,73b}, D. Ventura⁸⁶, M. Venturi¹⁶⁹, N. Venturi¹⁵⁸, A. Venturini²³,
 V. Vercesi^{121a}, M. Verducci^{132a,132b}, W. Verkerke¹⁰⁷, J.C. Vermeulen¹⁰⁷, A. Vest⁴⁴,
 M.C. Vetterli^{142,d}, O. Viazlo⁸¹, I. Vichou¹⁶⁵, T. Vickey¹³⁹, O.E. Vickey Boeriu¹³⁹,
 G.H.A. Viehhauser¹²⁰, S. Viel¹⁵, R. Vigne⁶², M. Villa^{20a,20b}, M. Villaplana Perez^{91a,91b},
 E. Vilucchi⁴⁷, M.G. Vincter²⁹, V.B. Vinogradov⁶⁵, I. Vivarelli¹⁴⁹, F. Vives Vaque³, S. Vlachos¹⁰,
 D. Vladoiu¹⁰⁰, M. Vlasak¹²⁸, M. Vogel^{32a}, P. Vokac¹²⁸, G. Volpi^{124a,124b}, M. Volpi⁸⁸,
 H. von der Schmitt¹⁰¹, H. von Radziewski⁴⁸, E. von Toerne²¹, V. Vorobel¹²⁹, K. Vorobev⁹⁸,
 M. Vos¹⁶⁷, R. Voss³⁰, J.H. Vosseveld⁷⁴, N. Vranjes¹³, M. Vranjes Milosavljevic¹³, V. Vrba¹²⁷,
 M. Vreeswijk¹⁰⁷, R. Vuillermet³⁰, I. Vukotic³¹, Z. Vykydal¹²⁸, P. Wagner²¹, W. Wagner¹⁷⁵,
 H. Wahlberg⁷¹, S. Wahrenmund⁴⁴, J. Wakabayashi¹⁰³, J. Walder⁷², R. Walker¹⁰⁰, W. Walkowiak¹⁴¹,
 C. Wang^{33c}, F. Wang¹⁷³, H. Wang¹⁵, H. Wang⁴⁰, J. Wang⁴², J. Wang^{33a}, K. Wang⁸⁷, R. Wang⁶,
 S.M. Wang¹⁵¹, T. Wang²¹, X. Wang¹⁷⁶, C. Wanotayaroj¹¹⁶, A. Warburton⁸⁷, C.P. Ward²⁸,
 D.R. Wardrope⁷⁸, M. Warsinsky⁴⁸, A. Washbrook⁴⁶, C. Wasicki⁴², P.M. Watkins¹⁸,
 A.T. Watson¹⁸, I.J. Watson¹⁵⁰, M.F. Watson¹⁸, G. Watts¹³⁸, S. Watts⁸⁴, B.M. Waugh⁷⁸,
 S. Webb⁸⁴, M.S. Weber¹⁷, S.W. Weber¹⁷⁴, J.S. Webster³¹, A.R. Weidberg¹²⁰, B. Weinert⁶¹,
 J. Weingarten⁵⁴, C. Weiser⁴⁸, H. Weits¹⁰⁷, P.S. Wells³⁰, T. Wenaus²⁵, T. Wengler³⁰, S. Wenig³⁰,
 N. Wermes²¹, M. Werner⁴⁸, P. Werner³⁰, M. Wessels^{58a}, J. Wetter¹⁶¹, K. Whalen¹¹⁶,
 A.M. Wharton⁷², A. White⁸, M.J. White¹, R. White^{32b}, S. White^{124a,124b}, D. Whiteson¹⁶³,
 F.J. Wickens¹³¹, W. Wiedenmann¹⁷³, M. Wielers¹³¹, P. Wienemann²¹, C. Wiglesworth³⁶,
 L.A.M. Wiik-Fuchs²¹, A. Wildauer¹⁰¹, H.G. Wilkens³⁰, H.H. Williams¹²², S. Williams¹⁰⁷,
 C. Willis⁹⁰, S. Willocq⁸⁶, A. Wilson⁸⁹, J.A. Wilson¹⁸, I. Wingerter-Seez⁵, F. Winklmeier¹¹⁶,
 B.T. Winter²¹, M. Wittgen¹⁴³, J. Wittkowski¹⁰⁰, S.J. Wollstadt⁸³, M.W. Wolter³⁹,
 H. Wolters^{126a,126c}, B.K. Wosiek³⁹, J. Wotschack³⁰, M.J. Woudstra⁸⁴, K.W. Wozniak³⁹, M. Wu⁵⁵,
 M. Wu³¹, S.L. Wu¹⁷³, X. Wu⁴⁹, Y. Wu⁸⁹, T.R. Wyatt⁸⁴, B.M. Wynne⁴⁶, S. Xella³⁶, D. Xu^{33a},
 L. Xu^{33b,aj}, B. Yabsley¹⁵⁰, S. Yacoub^{145b,ak}, R. Yakabe⁶⁷, M. Yamada⁶⁶, Y. Yamaguchi¹¹⁸,
 A. Yamamoto⁶⁶, S. Yamamoto¹⁵⁵, T. Yamanaka¹⁵⁵, K. Yamauchi¹⁰³, Y. Yamazaki⁶⁷, Z. Yan²²,
 H. Yang^{33e}, H. Yang¹⁷³, Y. Yang¹⁵¹, W-M. Yao¹⁵, Y. Yasu⁶⁶, E. Yatsenko⁵, K.H. Yau Wong²¹,
 J. Ye⁴⁰, S. Ye²⁵, I. Yeletsikh⁶⁵, A.L. Yen⁵⁷, E. Yildirim⁴², K. Yorita¹⁷¹, R. Yoshida⁶,
 K. Yoshihara¹²², C. Young¹⁴³, C.J.S. Young³⁰, S. Youssef²², D.R. Yu¹⁵, J. Yu⁸, J.M. Yu⁸⁹,
 J. Yu¹¹⁴, L. Yuan⁶⁷, A. Yurkewicz¹⁰⁸, I. Yusuff^{28,al}, B. Zabinski³⁹, R. Zaidan⁶³,
 A.M. Zaitsev^{130,aa}, J. Zalieckas¹⁴, A. Zaman¹⁴⁸, S. Zambito⁵⁷, L. Zanello^{132a,132b}, D. Zanzi⁸⁸,

C. Zeitnitz¹⁷⁵, M. Zeman¹²⁸, A. Zemla^{38a}, K. Zengel²³, O. Zenin¹³⁰, T. Ženiš^{144a}, D. Zerwas¹¹⁷, D. Zhang⁸⁹, F. Zhang¹⁷³, H. Zhang^{33c}, J. Zhang⁶, L. Zhang⁴⁸, R. Zhang^{33b}, X. Zhang^{33d}, Z. Zhang¹¹⁷, X. Zhao⁴⁰, Y. Zhao^{33d,117}, Z. Zhao^{33b}, A. Zhemchugov⁶⁵, J. Zhong¹²⁰, B. Zhou⁸⁹, C. Zhou⁴⁵, L. Zhou³⁵, L. Zhou⁴⁰, N. Zhou¹⁶³, C.G. Zhu^{33d}, H. Zhu^{33a}, J. Zhu⁸⁹, Y. Zhu^{33b}, X. Zhuang^{33a}, K. Zhukov⁹⁶, A. Zibell¹⁷⁴, D. Zieminska⁶¹, N.I. Zimine⁶⁵, C. Zimmermann⁸³, S. Zimmermann⁴⁸, Z. Zinonos⁵⁴, M. Zinser⁸³, M. Ziolkowski¹⁴¹, L. Živković¹³, G. Zobernig¹⁷³, A. Zoccoli^{20a,20b}, M. zur Nedden¹⁶, G. Zurzolo^{104a,104b}, L. Zwalinski³⁰.

¹ *Department of Physics, University of Adelaide, Adelaide, Australia*

² *Physics Department, SUNY Albany, Albany NY, United States of America*

³ *Department of Physics, University of Alberta, Edmonton AB, Canada*

⁴ ^(a) *Department of Physics, Ankara University, Ankara;* ^(c) *Istanbul Aydın University, Istanbul;* ^(d) *Division of Physics, TOBB University of Economics and Technology, Ankara, Turkey*

⁵ *LAPP, CNRS/IN2P3 and Université Savoie Mont Blanc, Annecy-le-Vieux, France*

⁶ *High Energy Physics Division, Argonne National Laboratory, Argonne IL, United States of America*

⁷ *Department of Physics, University of Arizona, Tucson AZ, United States of America*

⁸ *Department of Physics, The University of Texas at Arlington, Arlington TX, United States of America*

⁹ *Physics Department, University of Athens, Athens, Greece*

¹⁰ *Physics Department, National Technical University of Athens, Zografou, Greece*

¹¹ *Institute of Physics, Azerbaijan Academy of Sciences, Baku, Azerbaijan*

¹² *Institut de Física d'Altes Energies and Departament de Física de la Universitat Autònoma de Barcelona, Barcelona, Spain*

¹³ *Institute of Physics, University of Belgrade, Belgrade, Serbia*

¹⁴ *Department for Physics and Technology, University of Bergen, Bergen, Norway*

¹⁵ *Physics Division, Lawrence Berkeley National Laboratory and University of California, Berkeley CA, United States of America*

¹⁶ *Department of Physics, Humboldt University, Berlin, Germany*

¹⁷ *Albert Einstein Center for Fundamental Physics and Laboratory for High Energy Physics, University of Bern, Bern, Switzerland*

¹⁸ *School of Physics and Astronomy, University of Birmingham, Birmingham, United Kingdom*

¹⁹ ^(a) *Department of Physics, Bogazici University, Istanbul;* ^(b) *Department of Physics, Dogus University, Istanbul;* ^(c) *Department of Physics Engineering, Gaziantep University, Gaziantep, Turkey*

²⁰ ^(a) *INFN Sezione di Bologna;* ^(b) *Dipartimento di Fisica e Astronomia, Università di Bologna, Bologna, Italy*

²¹ *Physikalisches Institut, University of Bonn, Bonn, Germany*

²² *Department of Physics, Boston University, Boston MA, United States of America*

²³ *Department of Physics, Brandeis University, Waltham MA, United States of America*

²⁴ ^(a) *Universidade Federal do Rio De Janeiro COPPE/EE/IF, Rio de Janeiro;* ^(b) *Electrical Circuits Department, Federal University of Juiz de Fora (UFJF), Juiz de Fora;* ^(c) *Federal University of Sao Joao del Rei (UFSJ), Sao Joao del Rei;* ^(d) *Instituto de Física, Universidade de Sao Paulo, Sao Paulo, Brazil*

²⁵ *Physics Department, Brookhaven National Laboratory, Upton NY, United States of America*

- 26 (a) *National Institute of Physics and Nuclear Engineering, Bucharest*; (b) *National Institute for Research and Development of Isotopic and Molecular Technologies, Physics Department, Cluj Napoca*; (c) *University Politehnica Bucharest, Bucharest*; (d) *West University in Timisoara, Timisoara, Romania*
- 27 *Departamento de Física, Universidad de Buenos Aires, Buenos Aires, Argentina*
- 28 *Cavendish Laboratory, University of Cambridge, Cambridge, United Kingdom*
- 29 *Department of Physics, Carleton University, Ottawa ON, Canada*
- 30 *CERN, Geneva, Switzerland*
- 31 *Enrico Fermi Institute, University of Chicago, Chicago IL, United States of America*
- 32 (a) *Departamento de Física, Pontificia Universidad Católica de Chile, Santiago*; (b) *Departamento de Física, Universidad Técnica Federico Santa María, Valparaíso, Chile*
- 33 (a) *Institute of High Energy Physics, Chinese Academy of Sciences, Beijing*; (b) *Department of Modern Physics, University of Science and Technology of China, Anhui*; (c) *Department of Physics, Nanjing University, Jiangsu*; (d) *School of Physics, Shandong University, Shandong*; (e) *Department of Physics and Astronomy, Shanghai Key Laboratory for Particle Physics and Cosmology, Shanghai Jiao Tong University, Shanghai*; (f) *Physics Department, Tsinghua University, Beijing 100084, China*
- 34 *Laboratoire de Physique Corpusculaire, Clermont Université and Université Blaise Pascal and CNRS/IN2P3, Clermont-Ferrand, France*
- 35 *Nevis Laboratory, Columbia University, Irvington NY, United States of America*
- 36 *Niels Bohr Institute, University of Copenhagen, Kobenhavn, Denmark*
- 37 (a) *INFN Gruppo Collegato di Cosenza, Laboratori Nazionali di Frascati*; (b) *Dipartimento di Fisica, Università della Calabria, Rende, Italy*
- 38 (a) *AGH University of Science and Technology, Faculty of Physics and Applied Computer Science, Krakow*; (b) *Marian Smoluchowski Institute of Physics, Jagiellonian University, Krakow, Poland*
- 39 *Institute of Nuclear Physics Polish Academy of Sciences, Krakow, Poland*
- 40 *Physics Department, Southern Methodist University, Dallas TX, United States of America*
- 41 *Physics Department, University of Texas at Dallas, Richardson TX, United States of America*
- 42 *DESY, Hamburg and Zeuthen, Germany*
- 43 *Institut für Experimentelle Physik IV, Technische Universität Dortmund, Dortmund, Germany*
- 44 *Institut für Kern- und Teilchenphysik, Technische Universität Dresden, Dresden, Germany*
- 45 *Department of Physics, Duke University, Durham NC, United States of America*
- 46 *SUPA - School of Physics and Astronomy, University of Edinburgh, Edinburgh, United Kingdom*
- 47 *INFN Laboratori Nazionali di Frascati, Frascati, Italy*
- 48 *Fakultät für Mathematik und Physik, Albert-Ludwigs-Universität, Freiburg, Germany*
- 49 *Section de Physique, Université de Genève, Geneva, Switzerland*
- 50 (a) *INFN Sezione di Genova*; (b) *Dipartimento di Fisica, Università di Genova, Genova, Italy*
- 51 (a) *E. Andronikashvili Institute of Physics, Iv. Javakhishvili Tbilisi State University, Tbilisi*; (b) *High Energy Physics Institute, Tbilisi State University, Tbilisi, Georgia*
- 52 *II Physikalisches Institut, Justus-Liebig-Universität Giessen, Giessen, Germany*
- 53 *SUPA - School of Physics and Astronomy, University of Glasgow, Glasgow, United Kingdom*
- 54 *II Physikalisches Institut, Georg-August-Universität, Göttingen, Germany*
- 55 *Laboratoire de Physique Subatomique et de Cosmologie, Université Grenoble-Alpes, CNRS/IN2P3, Grenoble, France*

- ⁵⁶ *Department of Physics, Hampton University, Hampton VA, United States of America*
- ⁵⁷ *Laboratory for Particle Physics and Cosmology, Harvard University, Cambridge MA, United States of America*
- ⁵⁸ ^(a) *Kirchhoff-Institut für Physik, Ruprecht-Karls-Universität Heidelberg, Heidelberg;* ^(b) *Physikalisches Institut, Ruprecht-Karls-Universität Heidelberg, Heidelberg;* ^(c) *ZITI Institut für technische Informatik, Ruprecht-Karls-Universität Heidelberg, Mannheim, Germany*
- ⁵⁹ *Faculty of Applied Information Science, Hiroshima Institute of Technology, Hiroshima, Japan*
- ⁶⁰ ^(a) *Department of Physics, The Chinese University of Hong Kong, Shatin, N.T., Hong Kong;* ^(b) *Department of Physics, The University of Hong Kong, Hong Kong;* ^(c) *Department of Physics, The Hong Kong University of Science and Technology, Clear Water Bay, Kowloon, Hong Kong, China*
- ⁶¹ *Department of Physics, Indiana University, Bloomington IN, United States of America*
- ⁶² *Institut für Astro- und Teilchenphysik, Leopold-Franzens-Universität, Innsbruck, Austria*
- ⁶³ *University of Iowa, Iowa City IA, United States of America*
- ⁶⁴ *Department of Physics and Astronomy, Iowa State University, Ames IA, United States of America*
- ⁶⁵ *Joint Institute for Nuclear Research, JINR Dubna, Dubna, Russia*
- ⁶⁶ *KEK, High Energy Accelerator Research Organization, Tsukuba, Japan*
- ⁶⁷ *Graduate School of Science, Kobe University, Kobe, Japan*
- ⁶⁸ *Faculty of Science, Kyoto University, Kyoto, Japan*
- ⁶⁹ *Kyoto University of Education, Kyoto, Japan*
- ⁷⁰ *Department of Physics, Kyushu University, Fukuoka, Japan*
- ⁷¹ *Instituto de Física La Plata, Universidad Nacional de La Plata and CONICET, La Plata, Argentina*
- ⁷² *Physics Department, Lancaster University, Lancaster, United Kingdom*
- ⁷³ ^(a) *INFN Sezione di Lecce;* ^(b) *Dipartimento di Matematica e Fisica, Università del Salento, Lecce, Italy*
- ⁷⁴ *Oliver Lodge Laboratory, University of Liverpool, Liverpool, United Kingdom*
- ⁷⁵ *Department of Physics, Jožef Stefan Institute and University of Ljubljana, Ljubljana, Slovenia*
- ⁷⁶ *School of Physics and Astronomy, Queen Mary University of London, London, United Kingdom*
- ⁷⁷ *Department of Physics, Royal Holloway University of London, Surrey, United Kingdom*
- ⁷⁸ *Department of Physics and Astronomy, University College London, London, United Kingdom*
- ⁷⁹ *Louisiana Tech University, Ruston LA, United States of America*
- ⁸⁰ *Laboratoire de Physique Nucléaire et de Hautes Energies, UPMC and Université Paris-Diderot and CNRS/IN2P3, Paris, France*
- ⁸¹ *Fysiska institutionen, Lunds universitet, Lund, Sweden*
- ⁸² *Departamento de Física Teórica C-15, Universidad Autónoma de Madrid, Madrid, Spain*
- ⁸³ *Institut für Physik, Universität Mainz, Mainz, Germany*
- ⁸⁴ *School of Physics and Astronomy, University of Manchester, Manchester, United Kingdom*
- ⁸⁵ *CPPM, Aix-Marseille Université and CNRS/IN2P3, Marseille, France*
- ⁸⁶ *Department of Physics, University of Massachusetts, Amherst MA, United States of America*
- ⁸⁷ *Department of Physics, McGill University, Montreal QC, Canada*
- ⁸⁸ *School of Physics, University of Melbourne, Victoria, Australia*
- ⁸⁹ *Department of Physics, The University of Michigan, Ann Arbor MI, United States of America*
- ⁹⁰ *Department of Physics and Astronomy, Michigan State University, East Lansing MI, United States of America*

- 91 ^(a) *INFN Sezione di Milano*; ^(b) *Dipartimento di Fisica, Università di Milano, Milano, Italy*
- 92 *B.I. Stepanov Institute of Physics, National Academy of Sciences of Belarus, Minsk, Republic of Belarus*
- 93 *National Scientific and Educational Centre for Particle and High Energy Physics, Minsk, Republic of Belarus*
- 94 *Department of Physics, Massachusetts Institute of Technology, Cambridge MA, United States of America*
- 95 *Group of Particle Physics, University of Montreal, Montreal QC, Canada*
- 96 *P.N. Lebedev Institute of Physics, Academy of Sciences, Moscow, Russia*
- 97 *Institute for Theoretical and Experimental Physics (ITEP), Moscow, Russia*
- 98 *National Research Nuclear University MEPhI, Moscow, Russia*
- 99 *D.V. Skobeltsyn Institute of Nuclear Physics, M.V. Lomonosov Moscow State University, Moscow, Russia*
- 100 *Fakultät für Physik, Ludwig-Maximilians-Universität München, München, Germany*
- 101 *Max-Planck-Institut für Physik (Werner-Heisenberg-Institut), München, Germany*
- 102 *Nagasaki Institute of Applied Science, Nagasaki, Japan*
- 103 *Graduate School of Science and Kobayashi-Maskawa Institute, Nagoya University, Nagoya, Japan*
- 104 ^(a) *INFN Sezione di Napoli*; ^(b) *Dipartimento di Fisica, Università di Napoli, Napoli, Italy*
- 105 *Department of Physics and Astronomy, University of New Mexico, Albuquerque NM, United States of America*
- 106 *Institute for Mathematics, Astrophysics and Particle Physics, Radboud University Nijmegen/Nikhef, Nijmegen, Netherlands*
- 107 *Nikhef National Institute for Subatomic Physics and University of Amsterdam, Amsterdam, Netherlands*
- 108 *Department of Physics, Northern Illinois University, DeKalb IL, United States of America*
- 109 *Budker Institute of Nuclear Physics, SB RAS, Novosibirsk, Russia*
- 110 *Department of Physics, New York University, New York NY, United States of America*
- 111 *Ohio State University, Columbus OH, United States of America*
- 112 *Faculty of Science, Okayama University, Okayama, Japan*
- 113 *Homer L. Dodge Department of Physics and Astronomy, University of Oklahoma, Norman OK, United States of America*
- 114 *Department of Physics, Oklahoma State University, Stillwater OK, United States of America*
- 115 *Palacký University, RCPTM, Olomouc, Czech Republic*
- 116 *Center for High Energy Physics, University of Oregon, Eugene OR, United States of America*
- 117 *LAL, Université Paris-Sud and CNRS/IN2P3, Orsay, France*
- 118 *Graduate School of Science, Osaka University, Osaka, Japan*
- 119 *Department of Physics, University of Oslo, Oslo, Norway*
- 120 *Department of Physics, Oxford University, Oxford, United Kingdom*
- 121 ^(a) *INFN Sezione di Pavia*; ^(b) *Dipartimento di Fisica, Università di Pavia, Pavia, Italy*
- 122 *Department of Physics, University of Pennsylvania, Philadelphia PA, United States of America*
- 123 *National Research Centre “Kurchatov Institute” B.P.Konstantinov Petersburg Nuclear Physics Institute, St. Petersburg, Russia*

- 124 (a) *INFN Sezione di Pisa*; (b) *Dipartimento di Fisica E. Fermi, Università di Pisa, Pisa, Italy*
- 125 *Department of Physics and Astronomy, University of Pittsburgh, Pittsburgh PA, United States of America*
- 126 (a) *Laboratorio de Instrumentacao e Fisica Experimental de Particulas - LIP, Lisboa*; (b) *Faculdade de Ciências, Universidade de Lisboa, Lisboa*; (c) *Department of Physics, University of Coimbra, Coimbra*; (d) *Centro de Física Nuclear da Universidade de Lisboa, Lisboa*; (e) *Departamento de Física, Universidade do Minho, Braga*; (f) *Departamento de Física Teórica y del Cosmos and CAFPE, Universidad de Granada, Granada (Spain)*; (g) *Dep Física and CEFITEC of Faculdade de Ciências e Tecnologia, Universidade Nova de Lisboa, Caparica, Portugal*
- 127 *Institute of Physics, Academy of Sciences of the Czech Republic, Praha, Czech Republic*
- 128 *Czech Technical University in Prague, Praha, Czech Republic*
- 129 *Faculty of Mathematics and Physics, Charles University in Prague, Praha, Czech Republic*
- 130 *State Research Center Institute for High Energy Physics, Protvino, Russia*
- 131 *Particle Physics Department, Rutherford Appleton Laboratory, Didcot, United Kingdom*
- 132 (a) *INFN Sezione di Roma*; (b) *Dipartimento di Fisica, Sapienza Università di Roma, Roma, Italy*
- 133 (a) *INFN Sezione di Roma Tor Vergata*; (b) *Dipartimento di Fisica, Università di Roma Tor Vergata, Roma, Italy*
- 134 (a) *INFN Sezione di Roma Tre*; (b) *Dipartimento di Matematica e Fisica, Università Roma Tre, Roma, Italy*
- 135 (a) *Faculté des Sciences Ain Chock, Réseau Universitaire de Physique des Hautes Energies - Université Hassan II, Casablanca*; (b) *Centre National de l'Energie des Sciences Techniques Nucleaires, Rabat*; (c) *Faculté des Sciences Semlalia, Université Cadi Ayyad, LPHEA-Marrakech*; (d) *Faculté des Sciences, Université Mohamed Premier and LPTPM, Oujda*; (e) *Faculté des sciences, Université Mohammed V-Agdal, Rabat, Morocco*
- 136 *DSM/IRFU (Institut de Recherches sur les Lois Fondamentales de l'Univers), CEA Saclay (Commissariat à l'Energie Atomique et aux Energies Alternatives), Gif-sur-Yvette, France*
- 137 *Santa Cruz Institute for Particle Physics, University of California Santa Cruz, Santa Cruz CA, United States of America*
- 138 *Department of Physics, University of Washington, Seattle WA, United States of America*
- 139 *Department of Physics and Astronomy, University of Sheffield, Sheffield, United Kingdom*
- 140 *Department of Physics, Shinshu University, Nagano, Japan*
- 141 *Fachbereich Physik, Universität Siegen, Siegen, Germany*
- 142 *Department of Physics, Simon Fraser University, Burnaby BC, Canada*
- 143 *SLAC National Accelerator Laboratory, Stanford CA, United States of America*
- 144 (a) *Faculty of Mathematics, Physics & Informatics, Comenius University, Bratislava*; (b) *Department of Subnuclear Physics, Institute of Experimental Physics of the Slovak Academy of Sciences, Kosice, Slovak Republic*
- 145 (a) *Department of Physics, University of Cape Town, Cape Town*; (b) *Department of Physics, University of Johannesburg, Johannesburg*; (c) *School of Physics, University of the Witwatersrand, Johannesburg, South Africa*
- 146 (a) *Department of Physics, Stockholm University*; (b) *The Oskar Klein Centre, Stockholm, Sweden*
- 147 *Physics Department, Royal Institute of Technology, Stockholm, Sweden*
- 148 *Departments of Physics & Astronomy and Chemistry, Stony Brook University, Stony Brook NY, United States of America*
- 149 *Department of Physics and Astronomy, University of Sussex, Brighton, United Kingdom*

- ¹⁵⁰ *School of Physics, University of Sydney, Sydney, Australia*
- ¹⁵¹ *Institute of Physics, Academia Sinica, Taipei, Taiwan*
- ¹⁵² *Department of Physics, Technion: Israel Institute of Technology, Haifa, Israel*
- ¹⁵³ *Raymond and Beverly Sackler School of Physics and Astronomy, Tel Aviv University, Tel Aviv, Israel*
- ¹⁵⁴ *Department of Physics, Aristotle University of Thessaloniki, Thessaloniki, Greece*
- ¹⁵⁵ *International Center for Elementary Particle Physics and Department of Physics, The University of Tokyo, Tokyo, Japan*
- ¹⁵⁶ *Graduate School of Science and Technology, Tokyo Metropolitan University, Tokyo, Japan*
- ¹⁵⁷ *Department of Physics, Tokyo Institute of Technology, Tokyo, Japan*
- ¹⁵⁸ *Department of Physics, University of Toronto, Toronto ON, Canada*
- ¹⁵⁹ ^(a) *TRIUMF, Vancouver BC;* ^(b) *Department of Physics and Astronomy, York University, Toronto ON, Canada*
- ¹⁶⁰ *Faculty of Pure and Applied Sciences, University of Tsukuba, Tsukuba, Japan*
- ¹⁶¹ *Department of Physics and Astronomy, Tufts University, Medford MA, United States of America*
- ¹⁶² *Centro de Investigaciones, Universidad Antonio Narino, Bogota, Colombia*
- ¹⁶³ *Department of Physics and Astronomy, University of California Irvine, Irvine CA, United States of America*
- ¹⁶⁴ ^(a) *INFN Gruppo Collegato di Udine, Sezione di Trieste, Udine;* ^(b) *ICTP, Trieste;* ^(c) *Dipartimento di Chimica, Fisica e Ambiente, Università di Udine, Udine, Italy*
- ¹⁶⁵ *Department of Physics, University of Illinois, Urbana IL, United States of America*
- ¹⁶⁶ *Department of Physics and Astronomy, University of Uppsala, Uppsala, Sweden*
- ¹⁶⁷ *Instituto de Física Corpuscular (IFIC) and Departamento de Física Atómica, Molecular y Nuclear and Departamento de Ingeniería Electrónica and Instituto de Microelectrónica de Barcelona (IMB-CNM), University of Valencia and CSIC, Valencia, Spain*
- ¹⁶⁸ *Department of Physics, University of British Columbia, Vancouver BC, Canada*
- ¹⁶⁹ *Department of Physics and Astronomy, University of Victoria, Victoria BC, Canada*
- ¹⁷⁰ *Department of Physics, University of Warwick, Coventry, United Kingdom*
- ¹⁷¹ *Waseda University, Tokyo, Japan*
- ¹⁷² *Department of Particle Physics, The Weizmann Institute of Science, Rehovot, Israel*
- ¹⁷³ *Department of Physics, University of Wisconsin, Madison WI, United States of America*
- ¹⁷⁴ *Fakultät für Physik und Astronomie, Julius-Maximilians-Universität, Würzburg, Germany*
- ¹⁷⁵ *Fachbereich C Physik, Bergische Universität Wuppertal, Wuppertal, Germany*
- ¹⁷⁶ *Department of Physics, Yale University, New Haven CT, United States of America*
- ¹⁷⁷ *Yerevan Physics Institute, Yerevan, Armenia*
- ¹⁷⁸ *Centre de Calcul de l'Institut National de Physique Nucléaire et de Physique des Particules (IN2P3), Villeurbanne, France*
- ^a *Also at Department of Physics, King's College London, London, United Kingdom*
- ^b *Also at Institute of Physics, Azerbaijan Academy of Sciences, Baku, Azerbaijan*
- ^c *Also at Novosibirsk State University, Novosibirsk, Russia*
- ^d *Also at TRIUMF, Vancouver BC, Canada*
- ^e *Also at Department of Physics, California State University, Fresno CA, United States of America*

- ^f Also at Department of Physics, University of Fribourg, Fribourg, Switzerland
- ^g Also at Departamento de Física e Astronomia, Faculdade de Ciências, Universidade do Porto, Portugal
- ^h Also at Tomsk State University, Tomsk, Russia
- ⁱ Also at CPPM, Aix-Marseille Université and CNRS/IN2P3, Marseille, France
- ^j Also at Università di Napoli Parthenope, Napoli, Italy
- ^k Also at Institute of Particle Physics (IPP), Canada
- ^l Also at Particle Physics Department, Rutherford Appleton Laboratory, Didcot, United Kingdom
- ^m Also at Department of Physics, St. Petersburg State Polytechnical University, St. Petersburg, Russia
- ⁿ Also at Louisiana Tech University, Ruston LA, United States of America
- ^o Also at Institutio Catalana de Recerca i Estudis Avancats, ICREA, Barcelona, Spain
- ^p Also at Department of Physics, National Tsing Hua University, Taiwan
- ^q Also at Department of Physics, The University of Texas at Austin, Austin TX, United States of America
- ^r Also at Institute of Theoretical Physics, Iia State University, Tbilisi, Georgia
- ^s Also at CERN, Geneva, Switzerland
- ^t Also at Georgian Technical University (GTU), Tbilisi, Georgia
- ^u Also at O Chadai Academic Production, Ochanomizu University, Tokyo, Japan
- ^v Also at Manhattan College, New York NY, United States of America
- ^w Also at Institute of Physics, Academia Sinica, Taipei, Taiwan
- ^x Also at LAL, Université Paris-Sud and CNRS/IN2P3, Orsay, France
- ^y Also at Academia Sinica Grid Computing, Institute of Physics, Academia Sinica, Taipei, Taiwan
- ^z Also at School of Physics, Shandong University, Shandong, China
- ^{aa} Also at Moscow Institute of Physics and Technology State University, Dolgoprudny, Russia
- ^{ab} Also at section de Physique, Université de Genève, Geneva, Switzerland
- ^{ac} Also at International School for Advanced Studies (SISSA), Trieste, Italy
- ^{ad} Also at Department of Physics and Astronomy, University of South Carolina, Columbia SC, United States of America
- ^{ae} Also at School of Physics and Engineering, Sun Yat-sen University, Guangzhou, China
- ^{af} Also at Faculty of Physics, M.V.Lomonosov Moscow State University, Moscow, Russia
- ^{ag} Also at National Research Nuclear University MEPhI, Moscow, Russia
- ^{ah} Also at Department of Physics, Stanford University, Stanford CA, United States of America
- ^{ai} Also at Institute for Particle and Nuclear Physics, Wigner Research Centre for Physics, Budapest, Hungary
- ^{aj} Also at Department of Physics, The University of Michigan, Ann Arbor MI, United States of America
- ^{ak} Also at Discipline of Physics, University of KwaZulu-Natal, Durban, South Africa
- ^{al} Also at University of Malaya, Department of Physics, Kuala Lumpur, Malaysia
- * Deceased